actuators

Article

Predefined Time and Accuracy Adaptive Fault-Tolerant Control for Nonlinear Systems with Multiple Faults

Yakun Su [1,*], Yaling Jiang [1], Miao Tong [2] and Huanqing Wang [1]

[1] School of Mathematical Sciences, Bohai University, Jinzhou 121000, China; jiangyaling0726@163.com (Y.J.); ndwhq@163.com (H.W.)
[2] Marine Engineering College, Dalian Maritime University, Dalian 116000, China; mt19990315@163.com
* Correspondence: yasuyifan@163.com

Abstract: This work mainly studies the issue of predefined time and accuracy adaptive fault-tolerant control for strict-feedback nonlinear systems with multiple faults. The faults in the controlled system include actuator faults and external system faults. The unknown functions for nonlinear systems are approximated by fuzzy logic systems (FLSs). And then, according to the backstepping technique and the predefined time stability theory, an adaptive fuzzy control algorithm is presented, which can make sure that all closed-loop system signals remain predefined time bound and the tracking error converges to a predefined accuracy within the predefined time. Ultimately, the effectiveness of the presented control algorithm is proved through two simulation examples.

Keywords: adaptive fuzzy control; backstepping technique; fault-tolerant control; predefined time and accuracy; nonlinear systems

Citation: Su, Y.; Jiang, Y.; Tong, M.; Wang, H. Predefined Time and Accuracy Adaptive Fault-Tolerant Control for Nonlinear Systems with Multiple Faults. *Actuators* **2024**, *13*, 131. https://doi.org/10.3390/act13040131

Academic Editor: Guanghong Yang

Received: 8 March 2024
Revised: 29 March 2024
Accepted: 2 April 2024
Published: 5 April 2024

1. Introduction

For a long time in the past, the adaptive control problem of nonlinear systems has become a research hotspot. Experts and scholars have proposed many design methods for controllers, such as adaptive dynamic surface control [1], adaptive backstepping control [2], sliding mode control [3], and so on. Among these, the adaptive backstepping method can handle the uncertainty of nonlinear systems, so it is widely used, e.g., [4–6]. However, when there are complex and unknown nonlinear parts in the controlled system, it is very difficult to design a suitable controller solely using adaptive backstepping technology. Therefore, experts have proposed FLSs and neural networks (NNs) as commonly employed approximation tools, which can effectively solve the issue of model uncertainty in nonlinear systems in [7–14]. For example, the authors presented an adaptive controller for a class of high-order nonlinear systems with full state constraints and input saturation by combining FLSs and backstepping mechanisms in [15].

In fact, for practical control systems, actuator components are prone to malfunctions, which can affect the performance of the system, such as the ship autopilot [16], the one-link manipulator [17], the linear motor systems [18], etc. In order to solve this difficulty, experts have proposed many fault-tolerant control schemes [19–24]. An adaptive fault-tolerant control method for nonlinear systems with unmodeled dynamics and unknown control directions was proposed in [25]. In [26], a tuning function control scheme was presented for nonlinear systems with actuator or sensor faults and mismatched disturbances. In [27,28], some experts developed fault-tolerant control strategies for robot malfunctions. However, it is not comprehensive to only consider actuator faults. In reality, there are also external faults, so scholars have conducted research on fault-tolerant control problems with multiple faults, such as [29–32]. In [33], the authors studied the adaptive fault-tolerant control problem for stochastic nonlinear systems with multiple faults and full state constraints.

In the above analysis, only infinite-time fault-tolerant control was considered. However, in practical applications, the convergence time of the controlled system is often regarded as an important indicator for stability analysis. Scholars have conducted extensive research on the finite-time stability of nonlinear systems [34–38]. A finite-time adaptive fault-tolerant control strategy was proposed for nonlinear systems with multiple faults in [39]. Due to the fact that the settling time function of the finite-time stability theory depends on the initial conditions of the systems, the use of finite-time stability theory has limitations when the initial conditions are unknown. To solve this problem, experts have presented the fixed-time stability theory in [40]. After this, many significant milestones have been achieved [41–45]. In [46], an adaptive fixed-time fault-tolerant controller was presented for uncertain stochastic nonlinear systems with actuator and sensor faults. Due to the fact that the boundary of convergence time for the fixed-time stability theory is independent of the initial conditions of the control systems but limited by design parameters, the application of the fixed-time theory is limited when the bound function of convergence time is complex.

Thus, in order to overcome this difficult problem, scholars have presented the predefined time stability theory in [47], in which the upper boundary of its settling time is directly relevant to the controller parameters and is not associated with initial conditions. Because of the characteristics of predefined time stability theory, experts have presented many significant research results. In [48], an adaptive predefined time tracking control strategy was proposed for switched nonlinear systems. The author presented a predefined time adaptive tracking controller for nonlinear strict-feedback systems with time-varying output constraints in [49]. In [50], the authors proposed a class of Lyapunov-like conditions for dynamic systems based on predefined time stability. However, these research results did not consider the occurrence of faults and external faults in the control systems. This is the research motivation of this work.

Based on the above analysis, this paper designs an adaptive fuzzy controller with predefined time and accuracy for nonlinear systems with actuator faults and external faults. According to the predefined time stability theory, FLSs and the backstepping mechanism, an adaptive fuzzy controller is proposed to ensure that the tracking error meets the predefined accuracy and all signals in the closed-loop systems are bounded within the predefined time. The main innovation points of this study are as follows:

(1) Actuator faults and unknown external fault are concerned simultaneously for strict-feedback nonlinear systems for the first time under the predefined time and accuracy, and the predefined accuracy of general controlled systems was studied from different perspectives.

(2) An improved predefined accuracy condition is proposed to ensure the tracking error converges within the predefined neighborhood and avoid the "singularity problem" generated during virtual controller differentiation. By using FLSs to approximate the unknown functions of the controlled systems, the algorithm is optimized and the controller structure is simplified.

(3) Unlike [51], this work not only considers actuator faults but also external faults. And unlike [52], the piecewise function in the predefined accuracy condition proposed in this article is continuous.

The structure of the remaining of the article is as below. The problem formulations and preliminaries are proposed in Section 2. Section 3 contains the design and stability analysis of the controller. A numerical simulation example demonstrated the validity of the control strategy in Section 4. Section 5 provides the conclusion.

2. Problem Formulations and Preliminaries

2.1. Problem Formulation

Take into account the n-order nonlinear systems as outlined below:

$$\begin{cases} \dot{x}_i = f_i(\bar{x}_i) + g_i(\bar{x}_i)x_{i+1}, \quad i = 1, \dots, n-1 \\ \dot{x}_n = f_n(\bar{x}_n) + {g_n}^T(\bar{x}_n)u + H(t)\Gamma(x), \\ y = x_1, \end{cases} \tag{1}$$

where $\bar{x}_i = [x_1, \ldots, x_i]^T \in R^i (i = 1, 2, \ldots, n)$, $y \in R$ and $u = [u_1, u_2, \ldots, u_q] \in R^q$ are the state vector, system output and the control input, respectively; $g_i(\bar{x}_i)$ denotes the control gains, $g_n = [g_{n1}, g_{n2}, \ldots, g_{nq}]^T \in R^q$, and where $g_{nj}, j = 1, 2, \ldots, q$ is a known constant; $f_i(\bar{x}_i), i = 1, \ldots, n$ is the unknown smooth nonlinear function; $\Gamma(x)$ is the system external fault and the diagonal matrix $H(t) \in R^n$ is represented as

$$H(t) = \begin{cases} 1, & t \geq T_{fault} \\ 0, & t < T_{fault} \end{cases} \tag{2}$$

where T_{fault} is the time when the external fault occurred.

Remark 1. *The strict-feedback nonlinear systems, as classic controlled systems, have received widespread attention. A remarkable characteristic is that the i-th order function of the system is only related to the previous i system states. It can simulate actual industrial systems, such as a one-link manipulator, automotive control systems, and quadcopters. Meanwhile, strict-feedback nonlinear systems may have a wide range of uncertainties, which are not linearly parameterized, making modeling a challenging process. Therefore, it is meaningful to study the control method for strict-feedback nonlinear systems.*

Assumption 1. *For the gain function $g_i(\bar{x}_i), i = 1, 2, \ldots, n-1$ in systems (1), there are two known positive constants $\underline{g}_i$ and $\overline{g}_i$, which are the lower and upper bounds of $g_i(\bar{x}_i)$ and satisfy*

$$0 < \underline{g}_i \leq |g_i(\bar{x}_i)| \leq \overline{g}_i < \infty. \tag{3}$$

Assumption 2 ([53])**.** *The expected output tracking signal y_r and its i-th order derivative, $y_r^{(i)}$, $i = 1, 2, \ldots, n$ are continuous, known and bounded.*

2.2. Fault Description and Processing

In this article, the actuator faults considered include lock-in-place and loss-of-effectiveness [54,55].

(1) Lock-in-place model:

$$u_j(t) = \underline{u}_j, j \in \{j_1, \ldots, j_p\} \subset \{1, 2, \ldots, q\}, \tag{4}$$

where $\underline{u}_j$ is a constant expressing the lock-in-place fault; p is the number of actuators affected by lock-in-place faults.

(2) Loss-of-effectiveness model:

$$u_i(t) = \rho_i \nu_i(t), i \in \overline{\{j_1, \ldots, j_p\}} \subset \{1, 2, \ldots, q\}, \tag{5}$$

where $\nu_i(t)$ is the actual actuator signal; ρ_i is the fault ratio coeffcient; and $\underline{\rho}_i$ is the lower bound of ρ_i, which is an unknown constant that satisfies $\rho_i \in [\underline{\rho}_i, 1]$ and $0 < \underline{\rho}_i \leq 1$. When $\rho_i = 1$, there is no fault with the i-th actuator.

Remark 2. *The loss-of-effectiveness faults concerned in this article are widely present in practical control systems. Without external disturbances, the loss-of-effectiveness faults can occur due to long-term operation or mechanical wear, such as a one-link manipulator [16], aircraft systems [56] and autonomous underwater vehicles (AUVs) [57]. When actuator failure occurs, the controlled systems may collapse, and the considered fault may suddenly appear and enter the system without fault diagnosis information. Therefore, this fault is universal and has a wider range of applications.*

Then, based on (4) and (5), the input vector $u(t)$ of control systems can be represented as

$$u(t) = \rho\nu(t) + \zeta(\underline{u} - \rho\nu(t)), \tag{6}$$

where $\nu(t) = [\nu_1, \ldots, \nu_q(t)]^T$, $\underline{u} = [\underline{u}_1, \ldots, \underline{u}_q]^T$, $\rho = diag\{\rho_1, \ldots, \rho_q\}$ and $\zeta = diag\{\zeta_1, \ldots, \zeta_q\}$, where

$$\zeta_i = \begin{cases} 1, if the actuator faults as (4), i.e., \ u_i = \underline{u}_i \\ 0, otherwise. \end{cases} \tag{7}$$

The special control framework of the actuator is designed as shown below:

$$\nu_i(t) = \eta_i(x) u_0, \tag{8}$$

where u_0 is the input signal, and the gain function $\eta_i(x)$ has a lower bound $\underline{\eta}_i$ and an upper bound $\overline{\eta}_i$ for any $x \in R^n$, that is

$$0 < \underline{\eta}_i \leq \eta_i(x) \leq \overline{\eta}_i, i = 1, 2, \ldots, q. \tag{9}$$

2.3. Predefined Time Theory

A generic nonlinear system is outlined below:

$$\dot{x} = f(x; \aleph), \quad f(0; \aleph) = 0, \quad x_0 = x(0), \tag{10}$$

which assumes the origin is the equilibrium point; $x \in R^n$ indicates the state variable of systems (10); $\aleph \in R^b$ stands for the system parameter; and $f : R^n \to R^n$ is the nonlinear function.

Definition 1 ([58–60])**.** *The original point of system (10) satisfies the fixed-time stability theory, for* $\aleph$*, in which a constant* $T^* = T^*(\aleph) > 0$ *exists that holds* $\forall x_0 \in R^n$, $T(x_0) \leq T^*$ *for the settling-time function* $T : R^n \to R$. T^* *is known as a predefined time.*

Lemma 1 ([52])**.** *For the system (10), a Lyapunov function* $V(x)$ *satisfies*

$$\dot{V}(x) \leq -\frac{\pi}{rT_c}\left(V(x)^{1+\frac{r}{2}} + V(x)^{1-\frac{r}{2}}\right) + b, \tag{11}$$

in which $0 < r < 1$, $T_c > 0$ *and* $b > 0$ *are constants; then, the system (10) is practical predefined time stable, and* $V(x)$ *satisfies* $V(x) \leq \frac{rbT_c}{\pi}$ *in the predefined time* $2T_c$.

2.4. Fuzzy Logic Systems

The FLSs comprises the following rules: R^l: if x_1 is A_1^l and x_2 is A_2^l and ... and x_n is A_n^l, then y is $B^l, l = 1, 2, \ldots, N$, where $x = [x_1, \ldots, x_n]^T \in R^n$ is the FLSs input and $y \in R$ is the FLSs output. A_j^l and B^l are fuzzy sets, and N denotes the number of rules.

According to singleton funtion, center average defuzzification, and product inference [61], the FLSs can be indicated as

$$y(x) = \frac{\sum_{l=1}^{N} w_l \prod_{j=1}^{n} \mu_{A_j^l}(x_j)}{\sum_{l=1}^{N}\left[\prod_{j=1}^{n} \mu_{A_j^l}(x_j)\right]}, \tag{12}$$

where $w_l = max_{y \in R} \mu_{B^l(y)}$, $\mu_{A_j^l}(x_j)$ and $\mu_{B^l}(y)$ are the fuzzy membership functions of the fuzzy set A_j^l and B^l, respectively. The fuzzy basis function is defined as

$$s_l = \frac{\prod_{j=1}^{n} \mu_{A_j^l}(x_j)}{\sum_{l=1}^{N}\left[\prod_{j=1}^{n} \mu_{A_j^l}(x_j)\right]}, \tag{13}$$

where the fuzzy membership functions $\mu_{A_j^l}(x_j), \quad j = 1, \ldots, n$ are usually defined as Gaussian-type functions:

$$\mu_{A_j^l}(x_j) = \exp\left(\frac{-(x_j - \iota_j)^T (x_j - \iota_j)}{\tau_j^2}\right), \tag{14}$$

where $\iota_j = [\iota_{j1}, \ldots, \iota_{jn}]^T$ is the center of the basis function and τ_j is the width of the basis function.

The FLSs is represented as

$$y(x) = W^T S(x), \tag{15}$$

where $W = [w_1, \ldots, w_N]^T$, $S(x) = [s_1(x), \ldots, s_N(x)]^T$.

Lemma 2 ([61,62])**.** *For any positive constant ε, and any continuous function $f(x)$ defined in a compact set Δ, there exists an FLS that satisfies $\sup_{x \in \Delta} |f(x) - W^T S(x)| \leq \varepsilon$.*

Lemma 3 ([63])**.** *Assume $x_i \in R, i = 1, \ldots, n$ and $0 < c_1 \leq 1$, one has*

$$\sum_{i=1}^{n} |x_i|^{c_1} \geq \left(\sum_{i=1}^{n} |x_i|\right)^{c_1}. \tag{16}$$

Lemma 4 ([63])**.** *Assume $x_i \in R, i = 1, \ldots, n$ and $a_2 > 1$, we have*

$$\sum_{i=1}^{n} |x_i|^{a_2} \geq n^{1-a_2} \left(\sum_{i=1}^{n} |x_i|\right)^{a_2}. \tag{17}$$

Lemma 5 ([64])**.** *For $x \in R$ and $\forall \omega > 0$, we have*

$$0 \leq |x| \leq \omega + \frac{x^2}{\sqrt{x^2 + \omega^2}}. \tag{18}$$

Lemma 6 ([65])**.** *For real variables χ and ι, and any constants $a > 0$, $\kappa > 0$, we have*

$$|\chi|^a |\iota|^{1-a} \leq b\kappa |\chi| + (1-a)\kappa^{\frac{-a}{1-a}} |\iota|.$$

Lemma 7 ([66])**.** *For $0 \leq \beta \leq \gamma$, and $a > 1$, we have*

$$\beta(\gamma - \beta)^a \leq \frac{a}{a+1}(\gamma^{a+1} - \beta^{a+1}).$$

3. Adaptive Fuzzy Controller Design

In this section, we construct a predefined-time adaptive fault-tolerant control scheme to handle nonlinear controlled systems with actuator faults and external faults; the block diagram is shown in Figure 1.

Firstly, we set up the following coordinate transformations:

$$\begin{cases} z_1 = x_1 - y_r, \\ z_i = x_i - \alpha_{i-1}, \quad 2 \leq i \leq n-1 \end{cases} \tag{19}$$

in which $z_i (i = 1, \ldots, n)$ is the tracking error, $\alpha_{i-1} (i = 2, \ldots, n)$ is the virtual control signal, and y_r is the tracking signal. The process of controller design consists of n steps:

Step 1: Due to (1) and (19), the $\dot{z}_1$ is given as

$$
\begin{aligned}
\dot{z}_1 &= \dot{x}_1 - \dot{y}_r \\
&= f_1(\bar{x}_1) + g_1(\bar{x}_1)x_2 - \dot{y}_r \\
&= f_1(\bar{x}_1) + g_1(\bar{x}_1)(z_2 + \alpha_1) - \dot{y}_r.
\end{aligned} \tag{20}
$$

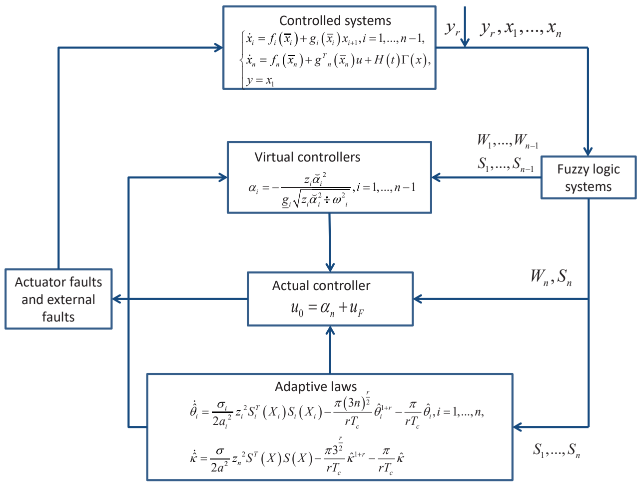

Figure 1. The block diagram of the predefined time adaptive fuzzy controller.

Select the following Lyapunov function

$$
V_1 = \frac{1}{2} z_1^2 + \frac{1}{2\sigma_1} \tilde{\theta}_1^2, \tag{21}
$$

in which $\tilde{\theta}_1 = \theta_1 - \hat{\theta}_1$, $\theta_1 = ||W_1||^2$ is estimated by $\hat{\theta}_1 > 0$, and the parameter $\sigma_1 > 0$ can be designed.

Then, the differentiation of V_1 produces

$$
\begin{aligned}
\dot{V}_1 &= z_1 \dot{z}_1 - \frac{1}{\sigma_1} \tilde{\theta}_1 \dot{\hat{\theta}}_1 \\
&= z_1 (f_1(\bar{x}_1) + g_1(\bar{x}_1)(z_2 + \alpha_1) - \dot{y}_r) - \frac{1}{\sigma_1} \tilde{\theta}_1 \dot{\hat{\theta}}_1 \\
&= z_1 (F_1 + g_1(\bar{x}_1)(z_2 + \alpha_1) - \frac{1}{2} z_1) - \frac{1}{\sigma_1} \tilde{\theta}_1 \dot{\hat{\theta}}_1,
\end{aligned} \tag{22}
$$

where $F_1 = f_1(\bar{x}_1) - \dot{y}_r + \frac{1}{2} z_1$.

Next, according to the definition of FLSs and Lemma 2, $W_1^T S_1(X_1)$ can be employed to approximate F_1; for $\varepsilon_1 > 0$, we have

$$
F_1 = W_1^T S_1(X_1) + \delta_1(X_1), \quad |\delta_1(X_1)| \leq \varepsilon_1, \tag{23}
$$

where $X_1 = [x_1, y_r, \dot{y}_r]^T$.

Then, by employing Young's inequality, we have

$$
\begin{aligned}
z_1 F_1 &= z_1 \left(W_1^T S_1(X_1) + \delta_1(X_1) \right) \\
&\leq |z_1| (||W_1|| ||S_1(X_1)|| + \varepsilon_1) \\
&\leq \frac{1}{2a_1^2} z_1^2 \theta_1 S_1^T(X_1) S_1(X_1) + \frac{a_1^2}{2} + \frac{z_1^2}{2} + \frac{\varepsilon_1^2}{2},
\end{aligned} \tag{24}
$$

where $a_1 > 0$ is a design parameter.

Then, substituting (24) into (22), $\dot{V}_1$ can be derived as

$$\begin{aligned} \dot{V}_1 &\le \frac{1}{2a_1^2} z_1^2 \hat{\theta}_1 S_1^T(X_1) S_1(X_1) + g_1 z_1 z_2 + g_1 z_1 \alpha_1 \\ & -\frac{1}{\sigma_1}\tilde{\theta}_1 \left(\dot{\hat{\theta}}_1 - \frac{\sigma_1}{2a_1^2} z_1^2 S_1^T(X_1) S_1(X_1) \right) + \frac{a_1^2}{2} + \frac{\varepsilon_1^2}{2}. \end{aligned} \tag{25}$$

The virtual controller α_1 and adaptive law $\hat{\theta}_1$ are selected as

$$\alpha_1 = -\frac{z_1 \check{\alpha}_1^2}{\underline{g}_1 \sqrt{z_1^2 \check{\alpha}_1^2 + \omega_1^2}}, \tag{26}$$

$$\dot{\hat{\theta}}_1 = \frac{\sigma_1}{2a_1^2} z_1^2 S_1^T(X_1) S_1(X_1) - \frac{\pi (3n)^{\frac{r}{2}}}{r T_c} \hat{\theta}_1^{1+r} - \frac{\pi}{r T_c} \hat{\theta}_1, \tag{27}$$

where $\omega_1 > 0$ is a small parameter and $\check{\alpha}_1$ is designed as

$$\check{\alpha}_1 = \frac{1}{2a_1^2} z_1 \hat{\theta}_1 S_1^T(X_1) S_1(X_1) + \frac{\pi (3n)^{\frac{r}{2}}}{r \lambda T_c} \left(\frac{1}{2} z_1^2 \right)^{1+\frac{r}{2}} + \frac{\pi}{2^{1-\frac{r}{2}} r \lambda T_c} \Phi_1, \tag{28}$$

where

$$\Phi_1 = \begin{cases} (z_1^2)^{1-\frac{r}{2}}, & |z_1| < \lambda \\ (1+pr)\lambda^{-3-r} z_1^5 - pr\lambda^{-1-r} z_1^3, & |z_1| \ge \lambda > 0 \end{cases} \tag{29}$$

where $\lambda > 0$ is predefined accuracy and $p > 0$ is a constant.

According to Lemma 5 and (26), one has

$$\begin{aligned} g_1 z_1 \alpha_1 &= -\frac{g_1 z_1^2 \check{\alpha}_1^2}{\underline{g}_1 \sqrt{z_1^2 \check{\alpha}_1^2 + \omega_1^2}} \\ &\le -\frac{z_1^2 \check{\alpha}_1^2}{\sqrt{z_1^2 \check{\alpha}_1^2 + \omega_1^2}} \\ &\le \omega_1 - |z_1 \check{\alpha}_1| \\ &\le \omega_1 - z_1 \check{\alpha}_1. \end{aligned} \tag{30}$$

(1) If $|z_1| \ge \lambda$, based on (28)–(30), we can obtain

$$\begin{aligned} -z_1 \check{\alpha}_1 &= -\frac{1}{2a_1^2} z_1^2 \hat{\theta}_1 S_1^T(X_1) S_1(X_1) - \frac{\pi (3n)^{\frac{r}{2}} z_1}{r \lambda T_c} \left(\frac{1}{2} z_1^2 \right)^{1+\frac{r}{2}} - \frac{\pi z_1}{2^{1-\frac{r}{2}} r \lambda T_c} \Phi_1 \\ &\le -\frac{1}{2a_1^2} z_1^2 \hat{\theta}_1 S_1^T(X_1) S_1(X_1) - \frac{\pi (3n)^{\frac{r}{2}}}{r T_c} \left(\frac{1}{2} z_1^2 \right)^{1+\frac{r}{2}} \\ & -\frac{\pi}{2^{1-\frac{r}{2}} r T_c} \left((1+pr)\lambda^{-3-r} z_1^5 - pr\lambda^{-1-r} z_1^3 \right) \\ &\le -\frac{1}{2a_1^2} z_1^2 \hat{\theta}_1 S_1^T(X_1) S_1(X_1) - \frac{\pi (3n)^{\frac{r}{2}}}{r T_c} \left(\frac{1}{2} z_1^2 \right)^{1+\frac{r}{2}} \\ & -\frac{\pi}{2^{1-\frac{r}{2}} r T_c} \left((1+pr)\lambda^{-1-r} z_1^3 - pr\lambda^{-1-r} z_1^3 \right) \\ &\le -\frac{1}{2a_1^2} z_1^2 \hat{\theta}_1 S_1^T(X_1) S_1(X_1) - \frac{\pi (3n)^{\frac{r}{2}}}{r T_c} \left(\frac{1}{2} z_1^2 \right)^{1+\frac{r}{2}} - \frac{\pi}{2^{1-\frac{r}{2}} r T_c} \lambda^{-1-r} z_1^3 \\ &\le -\frac{1}{2a_1^2} z_1^2 \hat{\theta}_1 S_1^T(X_1) S_1(X_1) - \frac{\pi (3n)^{\frac{r}{2}}}{r T_c} \left(\frac{1}{2} z_1^2 \right)^{1+\frac{r}{2}} - \frac{\pi}{r T_c} \left(\frac{1}{2} z_1^2 \right)^{1-\frac{r}{2}}. \end{aligned} \tag{31}$$

By employing Assumption 1, one can obtain

$$g_1 z_1 z_2 \le |\overline{g}_1 z_1 z_2|. \tag{32}$$

Then, substituting (26), (27) and (30)–(32) into (25) yields

$$\begin{aligned}\dot{V}_1 \le\ & \frac{1}{2a_1^2} z_1^2 \hat{\theta}_1 S_1^T(X_1) S_1(X_1) + g_1 z_1 z_2 + \omega_1 - z_1 \check{\alpha}_1 + \frac{\pi (3n)^{\frac{r}{2}}}{\sigma_1 r T_c} \tilde{\theta}_1 \hat{\theta}_1^{1+r} \\ & + \frac{\pi}{\sigma_1 r T_c} \tilde{\theta}_1 \hat{\theta}_1 + \frac{a_1^2}{2} + \frac{\varepsilon_1^2}{2} \\ \le\ & -\frac{\pi (3n)^{\frac{r}{2}}}{r T_c} \left(\frac{1}{2} z_1^2\right)^{1+\frac{r}{2}} - \frac{\pi}{r T_c} \left(\frac{1}{2} z_1^2\right)^{1-\frac{r}{2}} + \frac{\pi (3n)^{\frac{r}{2}}}{\sigma_1 r T_c} \tilde{\theta}_1 \hat{\theta}_1^{1+r} \\ & + \frac{\pi}{\sigma_1 r T_c} \tilde{\theta}_1 \hat{\theta}_1 + |\overline{g}_1 z_1 z_2| + b_1, \end{aligned} \tag{33}$$

where $b_1 = \omega_1 + \frac{a_1^2}{2} + \frac{\varepsilon_1^2}{2}$.

(2) If $|z_1| < \lambda$, the tracking error z_1 enters the predefined neighborhood, achieved the control, and from (28)–(30), one has

$$\begin{aligned} -z_1 \check{\alpha}_1 =\ & -\frac{1}{2a_1^2} z_1^2 \hat{\theta}_1 S_1^T(X_1) S_1(X_1) - \frac{\pi (3n)^{\frac{r}{2}} z_1}{r \lambda T_c} \left(\frac{1}{2} z_1^2\right)^{1+\frac{r}{2}} - \frac{\pi z_1}{2^{1-\frac{r}{2}} r \lambda T_c} \Phi_1 \\ \le\ & -\frac{1}{2a_1^2} z_1^2 \hat{\theta}_1 S_1^T(X_1) S_1(X_1) - \frac{\pi (3n)^{\frac{r}{2}}}{r T_c} \left(\frac{1}{2} z_1^2\right)^{1+\frac{r}{2}} - \frac{\pi}{r T_c} \left(\frac{1}{2} z_1^2\right)^{1-\frac{r}{2}}, \end{aligned} \tag{34}$$

we can see that the final derivation result of (34) is the same as that of (31). Therefore, for $|z_1| \ge \lambda$ and $|z_1| < \lambda$, we always have the following inequality that holds

$$\begin{aligned}\dot{V}_1 \le\ & -\frac{\pi (3n)^{\frac{r}{2}}}{r T_c} \left(\frac{1}{2} z_1^2\right)^{1+\frac{r}{2}} - \frac{\pi}{r T_c} \left(\frac{1}{2} z_1^2\right)^{1-\frac{r}{2}} + \frac{\pi (3n)^{\frac{r}{2}}}{\sigma_1 r T_c} \tilde{\theta}_1 \hat{\theta}_1^{1+r} + \frac{\pi}{\sigma_1 r T_c} \tilde{\theta}_1 \hat{\theta}_1 \\ & + |\overline{g}_1 z_1 z_2| + b_1. \end{aligned} \tag{35}$$

Step i $(i = 2, \ldots, n-1)$: From (1) and (19), $\dot{z}_i$ is

$$\begin{aligned} \dot{z}_i &= \dot{x}_i - \dot{\alpha}_{i-1} \\ &= f_i(\bar{x}_i) + g_i(\bar{x}_i) x_{i+1} - \dot{\alpha}_{i-1} \\ &= f_i(\bar{x}_i) + g_i(\bar{x}_i)(z_{i+1} + \alpha_i) - \dot{\alpha}_{i-1}. \end{aligned} \tag{36}$$

Consider the Lyapunov function as follows:

$$V_i = V_{i-1} + \frac{1}{2} z_i^2 + \frac{1}{2\sigma_i} \tilde{\theta}_i^2, \tag{37}$$

in which $\tilde{\theta}_i = \theta_i - \hat{\theta}_i$, $\theta_i = ||W_i||^2$ is estimated by $\hat{\theta}_i > 0$, and the parameter $\sigma_i > 0$ can be designed.

Then, we can obtain $\dot{V}_i$ as

$$\begin{aligned} \dot{V}_i &= \dot{V}_{i-1} + z_i \dot{z}_i - \frac{1}{\sigma_i} \tilde{\theta}_i \dot{\hat{\theta}}_i \\ &= \dot{V}_{i-1} + z_i (f_i(\bar{x}_i) + g_i(z_{i+1} + \alpha_i) - \dot{\alpha}_{i-1}) - \frac{1}{\sigma_i} \tilde{\theta}_i \dot{\hat{\theta}}_i \\ &= \dot{V}_{i-1} + z_i \left(F_i + g_i(z_{i+1} + \alpha_i) - \frac{1}{2} z_i\right) - \frac{1}{\sigma_i} \tilde{\theta}_i \dot{\hat{\theta}}_i, \end{aligned} \tag{38}$$

where $F_i = f_i(\bar{x}_i) - \dot{\alpha}_{i-1} + \frac{1}{2} z_i$.

Next, the FLSs $W^T S_i(X_i)$ are exploited to model F_i, and one can yield

$$F_i = W_i^T S_i(X_i) + \delta_i(X_i), \quad |\delta_i(X_i)| \leq \varepsilon_i, \tag{39}$$

where $\varepsilon_i > 0$ is given, $X_i = [x_1, \ldots, x_i, y_r, \dot{y}_r, \ldots, y_r^{(i)}]^T$.

Then, by utilizing Young's inequality, we can obtain

$$\begin{aligned} z_i F_i &= z_i \Big(W_i^T S_i(X_i) + \delta_i(X_i) \Big) \\ &\leq |z_i|(||W_i||||S_i(X_i)|| + \varepsilon_i) \\ &\leq \frac{1}{2a_i^2} z_i^2 \theta_i S_i^T(X_i) S_i(X_i) + \frac{a_i^2}{2} + \frac{z_i^2}{2} + \frac{\varepsilon_i^2}{2}, \end{aligned} \tag{40}$$

where $a_i > 0$ is a constant.

Substituting (40) into (38), one has

$$\begin{aligned} \dot{V}_i \leq \; & \dot{V}_{i-1} + \frac{1}{2a_i^2} z_i^2 \hat{\theta}_i S_i^T(X_i) S_i(X_i) + g_i z_i z_{i+1} + g_i z_i \alpha_i \\ & - \frac{1}{\sigma_i} \tilde{\theta}_i \left(\dot{\hat{\theta}}_i - \frac{\sigma_i}{2a_i^2} z_i^2 S_i^T(X_i) S_i(X_i) \right) + \frac{a_i^2}{2} + \frac{\varepsilon_i^2}{2}. \end{aligned} \tag{41}$$

Choose the virtual controller α_i and adaptive law $\hat{\theta}_i$ as

$$\alpha_i = -\frac{1}{\underline{g}_i} \left(\frac{z_i \check{\alpha}_i^2}{\sqrt{z_i^2 \check{\alpha}_i^2 + \omega_i^2}} + \frac{z_{i-1}^2 \bar{g}_{i-1}^2 z_i}{\sqrt{z_{i-1}^2 \bar{g}_{i-1}^2 z_i^2 + \omega_i^2}} \right), \tag{42}$$

$$\dot{\hat{\theta}}_i = \frac{\sigma_i}{2a_i^2} z_i^2 S_i^T(X_i) S_i(X_i) - \frac{\pi (3n)^{\frac{r}{2}}}{r T_c} \hat{\theta}_i^{1+r} - \frac{\pi}{r T_c} \hat{\theta}_i, \tag{43}$$

in which $\omega_i > 0$ is a small parameter and $\check{\alpha}_i$ is designed as

$$\check{\alpha}_i = \frac{1}{2a_i^2} z_i \hat{\theta}_i S_i^T(X_i) S_i(X_i) + \frac{\pi (3n)^{\frac{r}{2}}}{r \lambda T_c} \left(\frac{1}{2} z_i^2 \right)^{1+\frac{r}{2}} + \frac{\pi}{2^{1-\frac{r}{2}} r \lambda T_c} \Phi_i, \tag{44}$$

where

$$\Phi_i = \begin{cases} (z_i^2)^{1-\frac{r}{2}}, & |z_i| < \lambda \\ (1+pr)\lambda^{-3-r} z_i^5 - pr\lambda^{-1-r} z_i^3, & |z_i| \geq \lambda > 0 \end{cases} \tag{45}$$

According to Lemma 5 and (42), we have

$$\begin{aligned} g_i z_i \alpha_i &= -\frac{g_i z_i^2 \check{\alpha}_i^2}{\underline{g}_i \sqrt{z_i^2 \check{\alpha}_i^2 + \omega_i^2}} - \frac{g_i z_{i-1}^2 \bar{g}_{i-1}^2 z_i^2}{\underline{g}_i \sqrt{z_{i-1}^2 \bar{g}_{i-1}^2 z_i^2 + \omega_i^2}} \\ &\leq 2\omega_i - |z_i \check{\alpha}_i| - |\bar{g}_{i-1} z_{i-1} z_i| \\ &\leq 2\omega_i - z_i \check{\alpha}_i - |\bar{g}_{i-1} z_{i-1} z_i|. \end{aligned} \tag{46}$$

(1) If $|z_i| \geq \lambda > 0$, from (44)–(46) and similar to (31), one has

$$\begin{aligned} -z_i \check{\alpha}_i &= -\frac{1}{2a_i^2} z_i^2 \hat{\theta}_i S_i^T(X_i) S_i(X_i) - \frac{\pi (3n)^{\frac{r}{2}} z_i}{r \lambda T_c} \left(\frac{1}{2} z_i^2 \right)^{1+\frac{r}{2}} - \frac{\pi z_i}{2^{1-\frac{r}{2}} r \lambda T_c} \Phi_i \\ &\leq -\frac{1}{2a_i^2} z_i^2 \hat{\theta}_i S_i^T(X_i) S_i(X_i) - \frac{\pi (3n)^{\frac{r}{2}}}{r T_c} \left(\frac{1}{2} z_i^2 \right)^{1+\frac{r}{2}} - \frac{\pi}{r T_c} \left(\frac{1}{2} z_i^2 \right)^{1-\frac{r}{2}}. \end{aligned} \tag{47}$$

By utilizing Assumption 1, we can obtain

$$g_i z_i z_{i+1} \leq |\bar{g}_i z_i z_{i+1}|. \tag{48}$$

Then, bringing (42), (43) and (46)–(48) into (41), one has

$$\begin{aligned}
\dot{V}_i \leq\ & \dot{V}_{i-1} + \frac{1}{2a_i^2} z_i^2 \hat{\theta}_i S_i^T(X_i) S_i(X_i) + g_i z_i z_{i+1} + 2\omega_i - z_i \breve{\alpha}_i - |\bar{g}_{i-1} z_{i-1} z_i| \\
& + \frac{\pi (3n)^{\frac{r}{2}}}{\sigma_i r T_c} \tilde{\theta}_i \hat{\theta}_i^{1+r} + \frac{\pi}{\sigma_i r T_c} \tilde{\theta}_i \hat{\theta}_i + \frac{a_i^2}{2} + \frac{\varepsilon_i^2}{2} \\
\leq\ & -\sum_{j=1}^{i-1} \frac{\pi (3n)^{\frac{r}{2}}}{r T_c} \left(\frac{1}{2} z_j^2\right)^{1+\frac{r}{2}} - \sum_{j=1}^{i-1} \frac{\pi}{r T_c} \left(\frac{1}{2} z_j^2\right)^{1-\frac{r}{2}} + \sum_{j=1}^{i-1} \frac{\pi (3n)^{\frac{r}{2}}}{\sigma_j r T_c} \tilde{\theta}_j \hat{\theta}_j^{1+r} \\
& + \sum_{j=1}^{i-1} \frac{\pi}{\sigma_j r T_c} \tilde{\theta}_j \hat{\theta}_j + |\bar{g}_{-1} z_{i-1} z_i| - \frac{\pi (3n)^{\frac{r}{2}}}{r T_c} \left(\frac{1}{2} z_i^2\right)^{1+\frac{r}{2}} + b_{i-1} - \frac{\pi}{r T_c} \left(\frac{1}{2} z_i^2\right)^{1-\frac{r}{2}} \\
& + \frac{\pi (3n)^{\frac{r}{2}}}{\sigma_i r T_c} \tilde{\theta}_i \hat{\theta}_i^{1+r} + \frac{\pi}{\sigma_i r T_c} \tilde{\theta}_i \hat{\theta}_i + |\bar{g}_i z_i z_{i+1}| - |\bar{g}_{i-1} z_{i-1} z_i| + \frac{a_i^2}{2} + \frac{\varepsilon_i^2}{2} + 2\omega_i \\
\leq\ & -\sum_{j=1}^{i} \frac{\pi (3n)^{\frac{r}{2}}}{r T_c} \left(\frac{1}{2} z_j^2\right)^{1+\frac{r}{2}} - \sum_{j=1}^{i} \frac{\pi}{r T_c} \left(\frac{1}{2} z_j^2\right)^{1-\frac{r}{2}} + \sum_{j=1}^{i} \frac{\pi (3n)^{\frac{r}{2}}}{\sigma_j r T_c} \tilde{\theta}_j \hat{\theta}_j^{1+r} \\
& + \sum_{j=1}^{i} \frac{\pi}{\sigma_j r T_c} \tilde{\theta}_j \hat{\theta}_j + |\bar{g}_i z_i z_{i+1}| + b_i,
\end{aligned} \tag{49}$$

where $b_i = b_{i-1} + \frac{a_i^2}{2} + \frac{\varepsilon_i^2}{2} + 2\omega_i$.

(2) If $|z_i| < \lambda$, according to (44)–(46), we can obtain

$$\begin{aligned}
-z_i \breve{\alpha}_i =\ & -\frac{1}{2a_i^2} z_i^2 \hat{\theta}_i S_i^T(X_i) S_i(X_i) - \frac{\pi (3n)^{\frac{r}{2}} z_i}{r \lambda T_c} \left(\frac{1}{2} z_i^2\right)^{1+\frac{r}{2}} - \frac{\pi z_i}{2^{1-\frac{r}{2}} r \lambda T_c} \Phi_i \\
\leq\ & -\frac{1}{2a_i^2} z_i^2 \hat{\theta}_i S_i^T(X_i) S_i(X_i) - \frac{\pi (3n)^{\frac{r}{2}}}{r T_c} \left(\frac{1}{2} z_i^2\right)^{1+\frac{r}{2}} - \frac{\pi}{r T_c} \left(\frac{1}{2} z_i^2\right)^{1-\frac{r}{2}},
\end{aligned} \tag{50}$$

the inequality (50) is the same as inequality (47).

Therefore, based on the above derivation of situation (1) and situation (2), one has

$$\begin{aligned}
\dot{V}_i \leq\ & -\sum_{j=1}^{i} \frac{\pi (3n)^{\frac{r}{2}}}{r T_c} \left(\frac{1}{2} z_j^2\right)^{1+\frac{r}{2}} - \sum_{j=1}^{i} \frac{\pi}{r T_c} \left(\frac{1}{2} z_j^2\right)^{1-\frac{r}{2}} + \sum_{j=1}^{i} \frac{\pi (3n)^{\frac{r}{2}}}{\sigma_j r T_c} \tilde{\theta}_j \hat{\theta}_j^{1+r} \\
& + \sum_{j=1}^{i} \frac{\pi}{\sigma_j r T_c} \tilde{\theta}_j \hat{\theta}_j + |\bar{g}_i z_i z_{i+1}| + b_i.
\end{aligned} \tag{51}$$

Step n: The controller will be presented in this step. Similar to Step i, one can obtain $\dot{z}_n$:

$$\begin{aligned}
\dot{z}_n &= \dot{x}_n - \dot{\alpha}_{n-1} \\
&= f_n(\bar{x}_n) + g_n^T u + H(t)\Gamma(x) - \dot{\alpha}_{n-1}.
\end{aligned} \tag{52}$$

From (6) and (8), we have

$$\begin{aligned}
g_n^T u &= g_n^T(\rho v(t) + \zeta(\underline{u} - \rho v(t))) \\
&= g_n^T((1-\zeta)\rho v(t) + \zeta \underline{u}) \\
&= \sum_{j \neq j_1,\dots,j_p} \rho_j g_{nj} \eta_j u_0 + \sum_{j=j_1,\dots,j_p} g_{nj} \underline{u}_j \\
&= g_f u_0 + u_f,
\end{aligned} \tag{53}$$

where $g_f = \sum_{j \neq j_1,\ldots,j_p} \rho_j g_{nj} \eta_j$ and $u_f = \sum_{j=j_1,\ldots,j_p} g_{nj} \underline{u}_j$.

The Lyapunov function candidate function is chosen as shown below:

$$V_n = V_{n-1} + \frac{1}{2} z_n^2 + \frac{1}{2\sigma_n} \tilde{\theta}_n^2 + \frac{1}{2\sigma} \tilde{\kappa}^2, \tag{54}$$

where $\tilde{\theta}_n = \theta_n - \hat{\theta}_n$, $\tilde{\kappa} = \kappa - \hat{\kappa}$; $\theta_n = ||W_n||^2$ and $\kappa = ||W||^2$ are estimated by $\hat{\theta}_i > 0$ and $\hat{\kappa} > 0$; the parameters $\sigma_i > 0$ and $\sigma > 0$ can be designed.

Then, the time differentiation of V_n is

$$\begin{aligned} \dot{V}_n &= \dot{V}_{n-1} + z_n \dot{z}_n - \frac{1}{\sigma_n} \tilde{\theta}_n \dot{\hat{\theta}}_n - \frac{1}{\sigma} \tilde{\kappa} \dot{\hat{\kappa}} \\ &= \dot{V}_{n-1} + z_n (f_n(\bar{x}_n) + g_f u_0 + u_f + H(t)\Gamma(x) - \dot{\alpha}_{n-1}) - \frac{1}{\sigma_n} \tilde{\theta}_n \dot{\hat{\theta}}_n - \frac{1}{\sigma} \tilde{\kappa} \dot{\hat{\kappa}} \\ &= \dot{V}_{n-1} + z_n \Big(F_n + g_f u_0 + u_f + H(t)\Gamma(x) - z_n \Big) - \frac{1}{\sigma_n} \tilde{\theta}_n \dot{\hat{\theta}}_n - \frac{1}{\sigma} \tilde{\kappa} \dot{\hat{\kappa}}, \end{aligned} \tag{55}$$

where $F_n = f_n(\bar{x}_n) - \dot{\alpha}_{n-1} + z_n$.

Then, based on FLSs and Lemma 2, $W_n^T S_n(X_n)$ and $\Phi^T S(X)$ are used to model F_n and $\Gamma(x)$, respectively. For the given $\varepsilon_n > 0$ and $\bar{\delta} > 0$, we have

$$F_n = W_n^T S_n(X_n) + \delta_n(X_n), \quad |\delta_n(X_n)| \leq \varepsilon_n, \tag{56}$$

$$\Gamma(x) = \Phi^T S(X) + \delta(X), \quad |\delta(X)| \leq \bar{\delta}, \tag{57}$$

where $X_n = [x_1, \ldots, x_n, y_r, \dot{y}_r, \ldots, y_r^{(n)}]^T$, $X = [x_1, x_2, \ldots, x_n]^T$.

Then, by utilizing Young's inequality, it can be obtained that

$$z_n F_n \leq \frac{1}{2a_n^2} z_n^2 \theta_n S_n^T(X_n) S_n(X_n) + \frac{a_n^2}{2} + \frac{z_n^2}{2} + \frac{\varepsilon_n^2}{2}, \tag{58}$$

$$z_n H(t)\Gamma(x) \leq \frac{1}{2a^2} z_n^2 \kappa S^T(X) S(X) + \frac{a^2}{2} + \frac{z_n^2}{2} + \frac{\bar{\delta}^2}{2}, \tag{59}$$

where $a_n > 0$ and $a > 0$ are design constants.

Next, bringing (58) and (59) into (55), one can obtain

$$\begin{aligned} \dot{V}_n \leq\; & \dot{V}_{n-1} + \frac{1}{2a_n^2} z_n^2 \hat{\theta}_n S_n^T(X_n) S_n(X_n) + \frac{1}{2a^2} z_n^2 \hat{\kappa} S^T(X) S(X) + z_n \Big(g_f u_0 + u_f \Big) \\ & - \frac{1}{\sigma_n} \tilde{\theta}_n \left(\dot{\hat{\theta}}_n - \frac{\sigma_n}{2a_n^2} z_n^2 S_n^T(X_n) S_n(X_n) \right) - \frac{1}{\sigma} \tilde{\kappa} \Big(\dot{\hat{\kappa}} - \frac{\sigma}{2a^2} z_n^2 S^T(X) S(X) \Big) \\ & + \frac{a_n^2}{2} + \frac{\varepsilon_n^2}{2} + \frac{a^2}{2} + \frac{\bar{\delta}^2}{2}. \end{aligned} \tag{60}$$

We define the control law as

$$u_0 = \alpha_n + u_F, \tag{61}$$

in which

$$\alpha_n = -\frac{1}{g_f} \left(\frac{z_n \check{\alpha}_n^2}{\sqrt{z_n^2 \check{\alpha}_n^2 + \omega_n^2}} + \frac{z_{n-1}^2 \bar{g}_{n-1}^2 z_n}{\sqrt{z_{n-1}^2 \bar{g}_{n-1}^2 z_n^2 + \omega_n^2}} \right) - \frac{1}{g_f} u_f, \tag{62}$$

$$u_F = -\frac{1}{2 g_f a^2} \hat{\kappa} z_n S^T(X) S(X), \tag{63}$$

where $\omega_n > 0$ is a small parameter and $\check{\alpha}_n$ is selected as

$$\check{\alpha}_n = \frac{1}{2a_n^2} z_n \hat{\theta}_n S_n^T(X_n) S_n(X_n) + \frac{\pi(3n)^{\frac{r}{2}}}{r\lambda T_c}\left(\frac{1}{2}z_n^2\right)^{1+\frac{r}{2}} + \frac{\pi}{2^{1-\frac{r}{2}} r\lambda T_c}\Phi_n, \tag{64}$$

where Φ_n is designed as

$$\Phi_n = \begin{cases} (z_n^2)^{1-\frac{r}{2}}, & |z_n| < \lambda \\ (1+pr)\lambda^{-3-r} z_n^5 - pr\lambda^{-1-r} z_n^3, & |z_n| \geq \lambda > 0 \end{cases} \tag{65}$$

The adaptive law $\hat{\theta}_n$ and $\hat{\kappa}$ are constructed separately as

$$\dot{\hat{\theta}}_n = \frac{\sigma_n}{2a_n^2} z_n^2 S_n^T(X_n) S_n(X_n) - \frac{\pi(3n)^{\frac{r}{2}}}{rT_c}\hat{\theta}_n^{1+r} - \frac{\pi}{rT_c}\hat{\theta}_n, \tag{66}$$

$$\dot{\hat{\kappa}} = \frac{\sigma}{2a^2} z_n^2 S^T(X) S(X) - \frac{\pi 3^{\frac{r}{2}}}{rT_c}\hat{\kappa}^{1+r} - \frac{\pi}{rT_c}\hat{\kappa}. \tag{67}$$

According to (62), (63) and Lemma 5, we have

$$\begin{aligned} z_n g_f \alpha_n &\leq -\frac{z_n^2 \check{\alpha}_n^2}{\sqrt{z_n^2 \check{\alpha}_n^2 + \omega_n^2}} - \frac{z_{n-1}^2 \bar{g}_{n-1}^2 z_n^2}{\sqrt{z_{n-1}^2 \bar{g}_{n-1}^2 z_n^2 + \omega_n^2}} - z_n u_f \\ &\leq 2\omega_n - |z_n \check{\alpha}_n| - |\bar{g}_{n-1} z_{n-1} z_n| - z_n u_f \\ &\leq 2\omega_n - z_n \check{\alpha}_n - |\bar{g}_{n-1} z_{n-1} z_n| - z_n u_f, \end{aligned} \tag{68}$$

$$z_n g_f u_F \leq -\frac{1}{2a^2}\hat{\kappa} z_n^2 S^T(X) S(X). \tag{69}$$

Similar to Step i, when $|z_n| \geq \lambda > 0$ or $|z_n| < \lambda$, substituting (64)–(69) into (60) yields

$$\begin{aligned} \dot{V}_n \leq\ & \dot{V}_{n-1} + \frac{1}{2a_n^2} z_n^2 \hat{\theta}_n S_n^T(X_n) S_n(X_n) + 2\omega_n - z_n \check{\alpha}_n + \frac{1}{2a^2} z_n^2 \hat{\kappa} S^T(X) S(X) \\ & - |\bar{g}_{n-1} z_{n-1} z_n| + z_n g_f u_F + \frac{\pi(3n)^{\frac{r}{2}}}{\sigma_n r T_c}\tilde{\theta}_n \hat{\theta}_n^{1+r} + \frac{\pi}{\sigma_n r T_c}\tilde{\theta}_n \hat{\theta}_n + \frac{\pi 3^{\frac{r}{2}}}{\sigma r T_c}\tilde{\kappa}\hat{\kappa}^{1+r} \\ & + \frac{\pi}{\sigma r T_c}\tilde{\kappa}\hat{\kappa} + \frac{1}{2}a_n^2 + \frac{1}{2}\varepsilon_n^2 + \frac{1}{2}a^2 + \frac{1}{2}\bar{\delta}^2 \\ \leq\ & -\sum_{j=1}^{n-1} \frac{\pi(3n)^{\frac{r}{2}}}{rT_c}\left(\frac{1}{2}z_j^2\right)^{1+\frac{r}{2}} - \sum_{j=1}^{n-1} \frac{\pi}{rT_c}\left(\frac{1}{2}z_j^2\right)^{1-\frac{r}{2}} + \sum_{j=1}^{n-1} \frac{\pi(3n)^{\frac{r}{2}}}{\sigma_j r T_c}\tilde{\theta}_j \hat{\theta}_j^{1+r} + \sum_{j=1}^{n-1} \frac{\pi}{\sigma_j r T_c}\tilde{\theta}_j \hat{\theta}_j \\ & + |\bar{g}_{n-1} z_{n-1} z_n| + b_{n-1} - \frac{\pi(3n)^{\frac{r}{2}}}{rT_c}\left(\frac{1}{2}z_n^2\right)^{1+\frac{r}{2}} - \frac{\pi}{rT_c}\left(\frac{1}{2}z_n^2\right)^{1-\frac{r}{2}} - |\bar{g}_{n-1} z_{n-1} z_n| \\ & + \frac{\pi(3n)^{\frac{r}{2}}}{\sigma_n r T_c}\tilde{\theta}_n \hat{\theta}_n^{1+r} + \frac{\pi}{\sigma_n r T_c}\tilde{\theta}_n \hat{\theta}_n + \frac{\pi 3^{\frac{r}{2}}}{\sigma r T_c}\tilde{\kappa}\hat{\kappa}^{1+r} + \frac{\pi}{\sigma r T_c}\tilde{\kappa}\hat{\kappa} + \frac{a_n^2}{2} + \frac{\varepsilon_n^2}{2} + \frac{a^2}{2} + \frac{\bar{\delta}^2}{2} + 2\omega_n \\ \leq\ & -\sum_{j=1}^{n} \frac{\pi(3n)^{\frac{r}{2}}}{rT_c}\left(\frac{1}{2}z_j^2\right)^{1+\frac{r}{2}} - \sum_{j=1}^{n} \frac{\pi}{rT_c}\left(\frac{1}{2}z_j^2\right)^{1-\frac{r}{2}} + \sum_{j=1}^{n} \frac{\pi(3n)^{\frac{r}{2}}}{\sigma_j r T_c}\tilde{\theta}_j \hat{\theta}_j^{1+r} + \sum_{j=1}^{n} \frac{\pi}{\sigma_j r T_c}\tilde{\theta}_j \hat{\theta}_j \\ & + \frac{\pi 3^{\frac{r}{2}}}{\sigma r T_c}\tilde{\kappa}\hat{\kappa}^{1+r} + \frac{\pi}{\sigma r T_c}\tilde{\kappa}\hat{\kappa} + b_n, \end{aligned} \tag{70}$$

where $b_n = b_{n-1} + \frac{a_n^2}{2} + \frac{\varepsilon_n^2}{2} + \frac{a^2}{2} + \frac{\bar{\delta}^2}{2} + 2\omega_n$.

Theorem 1. *For the nonlinear systems (1) with actuator faults and external faults, when the virtual control signals (26), (42), the actual control (61) and the adaptive laws (27), (43), (66) and (67)* *are adopted. By designing appropriate parameters, all signals defined in these closed-loop systems maintain boundedness and z_1 will converge to a predefined accuracy λ within a predefined time $2T_c$.*

Proof of Theorem 1. According to Lemma 4, Lemma 7 and $0 < r < 1$, we can deduce that

$$\begin{aligned}\sum_{j=1}^{n}\frac{\pi(3n)^{\frac{r}{2}}}{\sigma_j r T_c}\tilde{\theta}_j\hat{\theta}_j^{1+r} &\leq \sum_{j=1}^{n}\frac{1+r}{2+r}\frac{\pi(3n)^{\frac{r}{2}}}{\sigma_j r T_c}\left(\theta_j{}^{2+r}-\tilde{\theta}_j^{2+r}\right)\\ &\leq \sum_{j=1}^{n}\frac{\pi(3n)^{\frac{r}{2}}}{\sigma_j r T_c}\left(\theta_j{}^{2+r}-\tilde{\theta}_j^{2+r}\right)\\ &\leq \sum_{j=1}^{n}\frac{\pi(3n)^{\frac{r}{2}}}{\sigma_j r T_c}\theta_j{}^{2+r}-\sum_{j=1}^{n}\frac{\pi 3^{\frac{r}{2}}}{rT_c}\left(\frac{\tilde{\theta}_j^2}{2\sigma_j}\right)^{1+\frac{r}{2}}. \end{aligned} \tag{71}$$

Similarly, it can be derived that

$$\frac{\pi 3^{\frac{r}{2}}}{\sigma r T_c}\tilde{\kappa}\hat{\kappa}^{1+r} \leq \frac{\pi 3^{\frac{r}{2}}}{\sigma r T_c}\kappa^{2+r}-\frac{\pi 3^{\frac{r}{2}}}{rT_c}\left(\frac{\tilde{\kappa}^2}{2\sigma}\right)^{1+\frac{r}{2}}. \tag{72}$$

By using Young's inequality, we have

$$\tilde{\theta}_j\hat{\theta}_j \leq \frac{1}{2}\theta_j{}^2-\frac{1}{2}\tilde{\theta}_j^2, \tag{73}$$

$$\tilde{\kappa}\hat{\kappa} \leq \frac{1}{2}\kappa^2-\frac{1}{2}\tilde{\kappa}^2. \tag{74}$$

Substituting (71)–(74) into (70) yields

$$\begin{aligned}\dot{V}_n \leq\; & -\sum_{j=1}^{n}\frac{\pi(3n)^{\frac{r}{2}}}{rT_c}\left(\frac{1}{2}z_j^2\right)^{1+\frac{r}{2}}-\sum_{j=1}^{n}\frac{\pi}{rT_c}\left(\frac{1}{2}z_j^2\right)^{1-\frac{r}{2}}-\sum_{j=1}^{n}\frac{\pi 3^{\frac{r}{2}}}{rT_c}\left(\frac{\tilde{\theta}_j^2}{2\sigma_j}\right)^{1+\frac{r}{2}}\\ & -\frac{\pi 3^{\frac{r}{2}}}{rT_c}\left(\frac{\tilde{\kappa}^2}{2\sigma}\right)^{1+\frac{r}{2}}-\sum_{j=1}^{n}\frac{\pi}{2\sigma_j r T_c}\tilde{\theta}_j^2-\frac{\pi}{2\sigma r T_c}\tilde{\kappa}^2+\frac{\pi}{rT_c}\left(\sum_{j=1}^{n}\frac{\tilde{\theta}_j^2}{2\sigma_j}\right)^{1-\frac{r}{2}}\\ & -\frac{\pi}{rT_c}\left(\sum_{j=1}^{n}\frac{\tilde{\theta}_j^2}{2\sigma_j}\right)^{1-\frac{r}{2}}+\frac{\pi}{rT_c}\left(\frac{\tilde{\kappa}^2}{2\sigma}\right)^{1-\frac{r}{2}}-\frac{\pi}{rT_c}\left(\frac{\tilde{\kappa}^2}{2\sigma}\right)^{1-\frac{r}{2}}+\sum_{j=1}^{n}\frac{\pi(3n)^{\frac{r}{2}}}{\sigma_j r T_c}\theta_j{}^{2+r}\\ & +\frac{\pi 3^{\frac{r}{2}}}{\sigma r T_c}\kappa^{2+r}+\sum_{j=1}^{n}\frac{\pi}{2\sigma_j r T_c}\theta_j^2+\frac{\pi}{2\sigma r T_c}\kappa^2+b_n. \end{aligned} \tag{75}$$

By using Lemma 6, one can obtain

$$\frac{\pi}{rT_c}\left(\sum_{j=1}^{n}\frac{\tilde{\theta}_j^2}{2\sigma_j}\right)^{1-\frac{r}{2}} \leq \frac{\pi}{rT_c}\sum_{j=1}^{n}\frac{\tilde{\theta}_j^2}{2\sigma_j}+\frac{\pi}{2T_c}\left(\frac{2}{2-r}\right)^{\frac{r-2}{r}}, \tag{76}$$

$$\frac{\pi}{rT_c}\left(\frac{\tilde{\eta}^2}{2\sigma}\right)^{1-\frac{r}{2}} \leq \frac{\pi}{rT_c}\frac{\tilde{\kappa}^2}{2\sigma}+\frac{\pi}{2T_c}\left(\frac{2}{2-r}\right)^{\frac{r-2}{r}}. \tag{77}$$

Based on Lemmas 3 and 4, we have

$$
\begin{aligned}
&-\sum_{j=1}^{n}\frac{\pi}{rT_c}\left(\frac{1}{2}z_j^2\right)^{1-\frac{r}{2}}-\frac{\pi}{rT_c}\left(\sum_{j=1}^{n}\frac{\tilde{\theta}_j^2}{2\sigma_j}\right)^{1-\frac{r}{2}}-\frac{\pi}{rT_c}\left(\frac{\tilde{\kappa}^2}{2\sigma}\right)^{1-\frac{r}{2}}\\
\leq\ & -\frac{\pi}{rT_c}\left[\sum_{j=1}^{n}\frac{1}{2}z_j^2+\sum_{j=1}^{n}\frac{\tilde{\theta}_j^2}{2\sigma_j}+\frac{\tilde{\kappa}^2}{2\sigma}\right]^{1-\frac{r}{2}}, \qquad (78)
\end{aligned}
$$

$$
\begin{aligned}
&-\sum_{j=1}^{n}\frac{\pi(3n)^{\frac{r}{2}}}{rT_c}\left(\frac{1}{2}z_j^2\right)^{1+\frac{r}{2}}-\sum_{j=1}^{n}\frac{\pi 3^{\frac{r}{2}}}{rT_c}\left(\frac{\tilde{\theta}_j^2}{2\sigma_j}\right)^{1+\frac{r}{2}}-\frac{\pi 3^{\frac{r}{2}}}{rT_c}\left(\frac{\tilde{\kappa}^2}{2\sigma}\right)^{1+\frac{r}{2}}\\
\leq\ & -\frac{\pi}{rT_c}\left[\sum_{j=1}^{n}\frac{1}{2}z_j^2+\sum_{j=1}^{n}\frac{\tilde{\theta}_j^2}{2\sigma_j}+\frac{\tilde{\kappa}^2}{2\sigma}\right]^{1+\frac{r}{2}}. \qquad (79)
\end{aligned}
$$

Substituting (76)–(79) into (75), one has

$$
\begin{aligned}
\dot{V}_n \leq\ & -\frac{\pi}{rT_c}\left[\sum_{j=1}^{n}\frac{1}{2}z_j^2+\sum_{j=1}^{n}\frac{\tilde{\theta}_j^2}{2\sigma_j}+\frac{\tilde{\kappa}^2}{2\sigma}\right]^{1+\frac{r}{2}}-\frac{\pi}{rT_c}\left[\sum_{j=1}^{n}\frac{1}{2}z_j^2+\sum_{j=1}^{n}\frac{\tilde{\theta}_j^2}{2\sigma_j}+\frac{\tilde{\kappa}^2}{2\sigma}\right]^{1-\frac{r}{2}}\\
&+\sum_{j=1}^{n}\frac{\pi(3n)^{\frac{r}{2}}}{\sigma_j rT_c}\theta_j^{2+r}+\frac{\pi 3^{\frac{r}{2}}}{\sigma rT_c}\kappa^{2+r}+\frac{\pi}{T_c}\left(\frac{2}{2-r}\right)^{\frac{r-2}{r}}+\sum_{j=1}^{n}\frac{\pi}{2\sigma_j rT_c}\theta_j^2\\
&+\frac{\pi}{2\sigma rT_c}\kappa^2+b_n\\
\leq\ & -\frac{\pi}{rT_c}\left(V_n^{1+\frac{r}{2}}+V_n^{1-\frac{r}{2}}\right)+b, \qquad (80)
\end{aligned}
$$

where $b=\sum_{j=1}^{n}\frac{\pi(3n)^{\frac{r}{2}}}{\sigma_j rT_c}\theta_j^{2+r}+\frac{\pi 3^{\frac{r}{2}}}{\sigma rT_c}\kappa^{2+r}+\frac{\pi}{T_c}\left(\frac{2}{2-r}\right)^{\frac{r-2}{r}}+\sum_{j=1}^{n}\frac{\pi}{2\sigma_j rT_c}\theta_j^2+\frac{\pi}{2\sigma rT_c}\kappa^2+b_n$.

Therefore, when $|z_i|\geq\lambda$ or $|z_i|<\lambda$, we can both obtain

$$
\dot{V}_n=-\frac{\pi}{rT_c}\left(V_n^{1+\frac{r}{2}}+V_n^{1-\frac{r}{2}}\right)+b. \qquad (81)
$$

From Lemma 1, we have

$$
|z_1|\leq\sqrt{\frac{2rbT_c}{\pi}}, \qquad (82)
$$

this means that z_1 is bounded within the predefined-time $2T_c$.

And then based on (54), (81) and Lemma 1, we can deduce that V_n, $\tilde{\theta}_i$ and $\tilde{\kappa}$ are bounded, and z_i satisfies $|z_i|\leq\lambda$ within predefined time $2T_c$. According to Assumption 2 and the boundedness of z_1, we can see that x_1 is bounded. Because θ_i is a constant and $\tilde{\theta}_i$ is bounded, we can obtain that $\hat{\theta}_i$ is bounded. Due to the boundedness of $\tilde{\kappa}$ and the constant κ, we can deduce that $\hat{\kappa}$ is bounded. Since z_i and $\alpha_{i-1}, i=2,\ldots,n$ are bounded from (26) and (42), so the boundedness of x_i follows from $x_i=z_i+\alpha_{i-1}$. On the basis of the above discussion and analysis, all signals of the closed-loop systems maintain boundedness. This completes the proof. □

4. Simulation

Example 1. *Consider a second-order strict feedback nonlinear system as outlined below:*

$$
\begin{cases}
\dot{x}_1=f_1(\bar{x}_1)+g_1(\bar{x}_1)x_2,\\
\dot{x}_2=f_2(\bar{x}_2)+g_2^T u+H(t)\Gamma(x),\\
y=x_1,
\end{cases} \qquad (83)
$$

where $f_1(\bar{x}_1) = x_1^2 \cos(x_1)$, $g_1(\bar{x}_1) = 2 + x_1^2$, $f_2(\bar{x}_2) = x_1 \cos(x_1 x_2) - x_1^2 x_2 e^{x_2}$, $g_2 = [g_{2_1}, g_{2_2}]^T$ *and* $u = [u_1, u_2]$.

The virtual control signal α_1 *and the actual controller* u_0 *are constructed as shown below:*

$$\alpha_1 = -\frac{z_1 \breve{\alpha}_1^2}{\underline{g}_1 \sqrt{z_1^2 \breve{\alpha}_1^2 + \omega_1^2}}, \tag{84}$$

$$\begin{aligned} u_0 &= \alpha_2 + u_F \\ &= -\frac{1}{g_f}\left(\frac{z_2 \breve{\alpha}_2^2}{\sqrt{z_2^2 \breve{\alpha}_2^2 + \omega_2^2}} + \frac{z_1^2 \bar{g}_1^2 z_2}{\sqrt{z_1^2 \bar{g}_1^2 z_2^2 + \omega_2^2}} + u_f + \frac{1}{2a^2} \hat{\kappa} z_2 S^T(X) S(X)\right). \end{aligned} \tag{85}$$

The adaptive laws are constructed as shown below:

$$\dot{\hat{\theta}}_1 = \frac{\sigma_1}{2a_1^2} z_1^2 S_1^T(X_1) S_1(X_1) - \frac{\pi (3n)^{\frac{r}{2}}}{r T_c} \hat{\theta}_1^{1+r} - \frac{\pi}{r T_c} \hat{\theta}_1, \tag{86}$$

$$\dot{\hat{\theta}}_2 = \frac{\sigma_2}{2a_2^2} z_2^2 S_2^T(X_2) S_2(X_2) - \frac{\pi (3n)^{\frac{r}{2}}}{r T_c} \hat{\theta}_2^{1+r} - \frac{\pi}{r T_c} \hat{\theta}_2, \tag{87}$$

$$\dot{\hat{\kappa}} = \frac{\sigma}{2a^2} z_2^2 S^T(X) S(X) - \frac{\pi 3^{\frac{r}{2}}}{r T_c} \hat{\kappa}^{1+r} - \frac{\pi}{r T_c} \hat{\kappa}. \tag{88}$$

The block diagram of a predefined-time adaptive fuzzy controller is shown in Figure 2.

The initial conditions and parameters of the controlled system (83) are presented in Table 1. Three sets of predefined time are set to $2T_c = 2$, $2T_c = 4$ *and* $2T_c = 6$. *The reference signal is selected as* $y_r = 0.5(\sin(0.5t) - \sin(t))$. *The actuator faults are set to* $u_1 = 0.6v_1$ *and* $u_2 = \bar{u}_2 = 10$ *for* $t \geq 7$ *s, and the external fault occurs at* $T_{fault} = 15$ *s.*

The simulation results are presented in Figures 3–7. Figure 3 represents the system output y *and the tracking signal* y_r. *Figure 4 shows the trajectory of the tracking error* z_1. *Figure 5 displays the trajectory of the system state* x_2. *Figure 6 displays the trajectories of the actual control inputs* u_1 *and* u_2. *Figure 7 is the curves of adaptive parameters* $\hat{\theta}_1$, $\hat{\theta}_2$ *and* $\hat{\kappa}$. *Based on the simulation results, we can draw the conclusion that all the closed-loop system signals remain bounded and the tracking error can converge to a predefined accuracy within the predefined time.*

Table 1. Parameters of simulation Example 1.

Parameters	Value	Parameters	Value
$x_1(0)$	0.05	$x_2(0)$	0.02
n	2	p	0.1
g_{2_1}	1	g_{2_1}	1
r	0.35	$\underline{g}_1$	1
$\bar{g}_1$	3	ω_1	0.3
ω_2	0.3	a_1	5
a_2	5	a	5
σ_1	5	σ_2	1.5
σ	1.5	λ	0.1

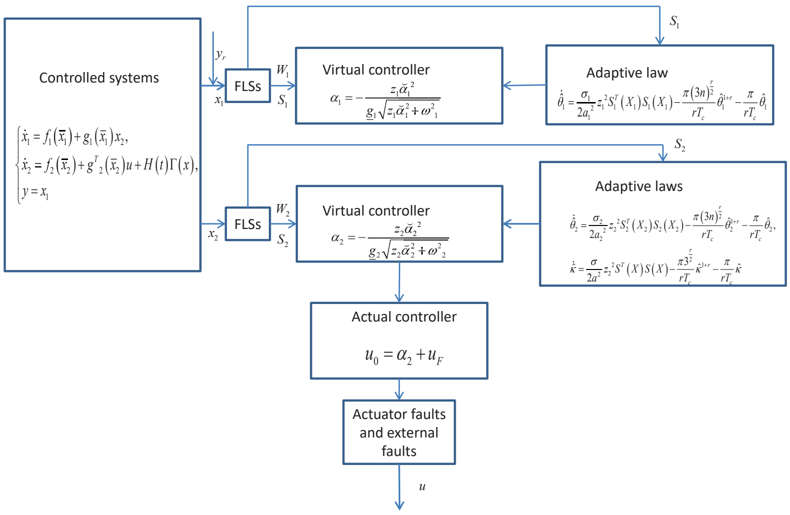

Figure 2. The block diagram of predefined time adaptive fuzzy controller for Example 1.

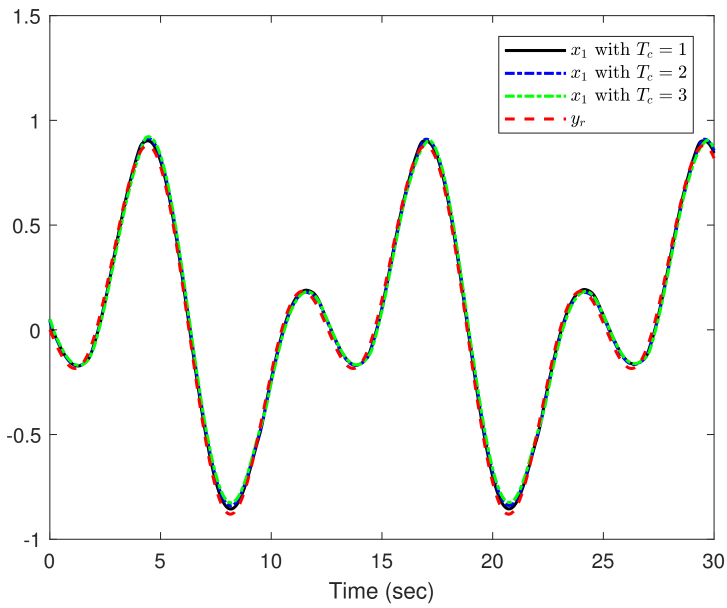

Figure 3. System output y and reference signal y_r of Example 1.

Example 2. *For the one-link manipulator with multiple faults:*

$$\begin{cases} D\ddot{q} + B\dot{q} + N\sin(q) = \tau \\ M\dot{\tau} + H\tau = g^T u + H(t)\Gamma(x) - K_m\dot{q}, \end{cases} \tag{89}$$

where q stands for the link position, $\dot{q}$ expresses the velocity, and $\ddot{q}$ is the acceleration; τ is the torque produced by the motor and $u = [u_1, u_2]$ is the control input with multiple faults. The parameters are selected to $D = B = M = 1$, $N = H = 10$, $K_m = 2$. Then, we make $x_1 = q$, $x_2 = \dot{q} = \dot{x}_1$ and $x_3 = \tau$, and the system (89) can be rewritten as

$$\begin{cases} \dot{x}_1 = f_1(\bar{x}_1) + g_1(\bar{x}_1)x_2 \\ \dot{x}_2 = f_2(\bar{x}_2) + g_2(\bar{x}_2)x_3 \\ \dot{x}_3 = f_3(\bar{x}_3) + g^T u + H(t)\Gamma(x) \\ y = x_1 \end{cases} \tag{90}$$

where $g_1(\bar{x}_1) = g_2(\bar{x}_2) = 1$, $g = [1,2]^T$, $f_1(\bar{x}_1) = 0$, $f_2(\bar{x}_2) = -x_2 - 10\sin(x_1) + x_1^2\cos(x_2)$, $f_3(\bar{x}_3) = -2x_2 - 10x_3$.

The block diagram of predefined-time adaptive fuzzy controller is diplayed in Figure 8.

The initial values and adjustable parameters of (90) are represented in Table 2. The predefined times are set to $2T_c = 4$ *and* $2T_c = 6$*. The reference signal is* $y_r = 0.5(\sin(0.5t) - \sin(t))$*. The actuator faults are set to* $u_1 = 0.6v_1$ *and* $u_2 = \bar{u}_2 = 15$ *for* $t \geq 5$ *s, and the external fault occurs at* $T_{fault} = 10$ *s.*

The simulation results are shown in Figures 9–13, in which the system output y *and tracking signal* y_r *are represented in Figure 9, Figure 10 displays the tracking error* z_1*, Figure 11 is the trajectory of the system states* x_2 *and* x_3*, actual control inputs* u_1 *and* u_2 *are displayed in Figure 12, and Figure 13 expresses the curves of adaptive parameters* $\hat{\theta}_1$*,* $\hat{\theta}_2$*,* $\hat{\theta}_3$ *and* $\hat{\kappa}$*. According to the results, we can conclude that all the closed-loop system signals meet the predefined time-bound conditions and the tracking error can converge to a predefined neighborhood.*

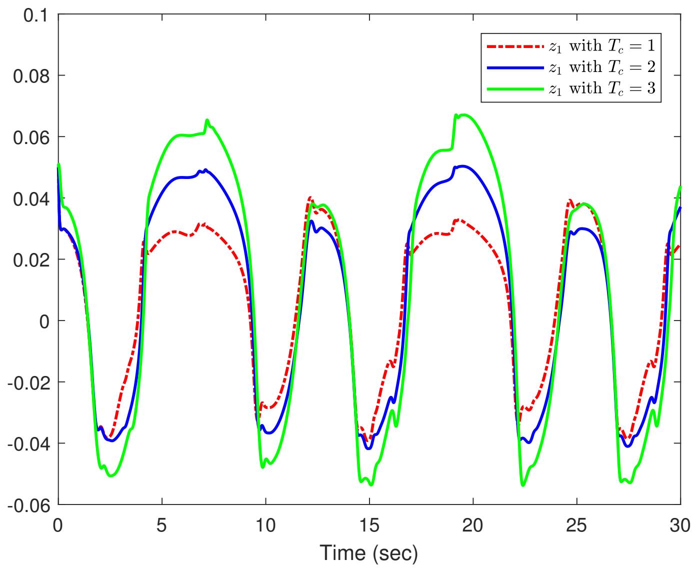

Figure 4. Tracking error z_1 of Example 1.

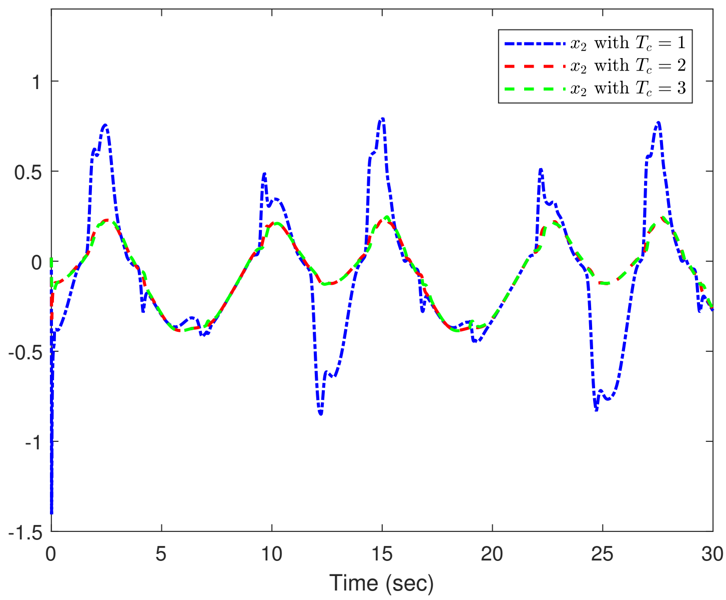

Figure 5. State variable x_2 of Example 1.

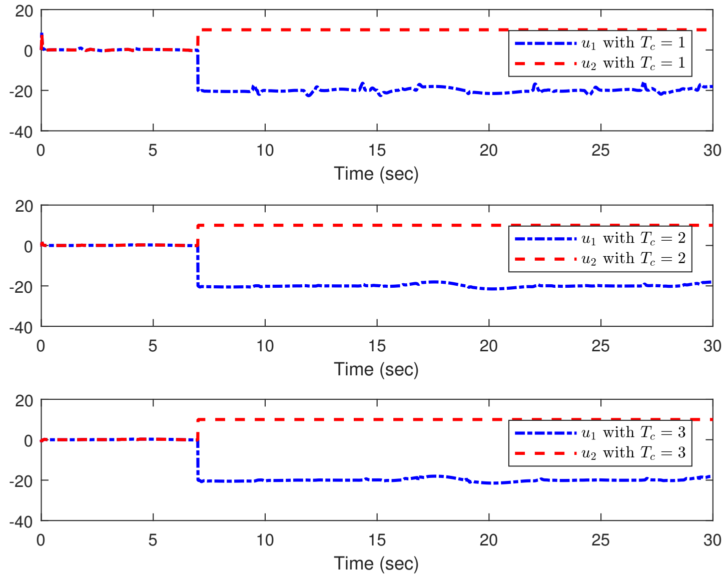

Figure 6. The actual control inputs u_1 and u_2 of Example 1.

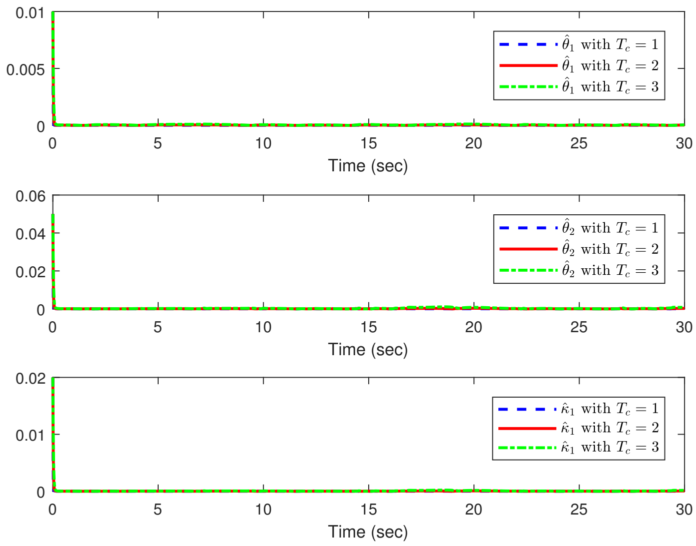

Figure 7. Adaptive laws $\hat{\theta}_1$, $\hat{\theta}_2$ and $\hat{\kappa}$.

Table 2. Parameters of simulation Example 2.

Parameters	Value	Parameters	Value
$x_1(0)$	0.01	$x_2(0)$	0.02
$x_3(0)$	0.01	n	3
p	10	g_{3_1}	1
g_{3_2}	2	r	0.1
$\underline{g}_1$	1	$\bar{g}_1$	1
ω_1	0.1	ω_2	0.1
a_1	1	a_2	1
a_3	1	a	1.5
σ_1	5	σ_2	10
σ_3	10	σ	10
λ	0.15		

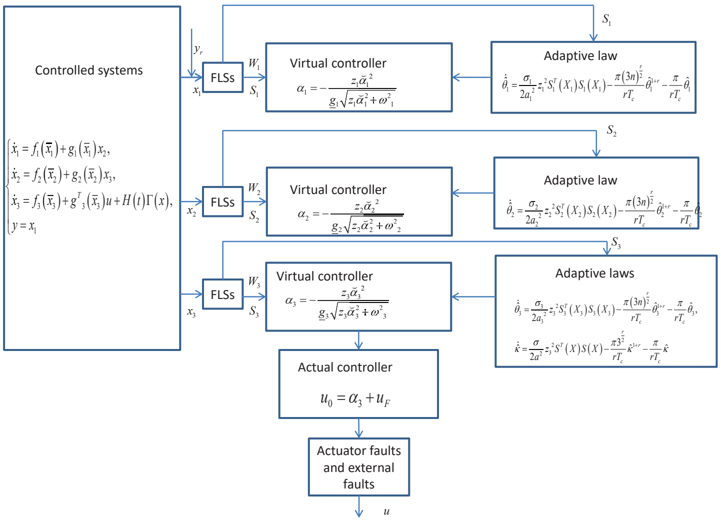

Figure 8. The block diagram of predefined time adaptive fuzzy controller for Example 2.

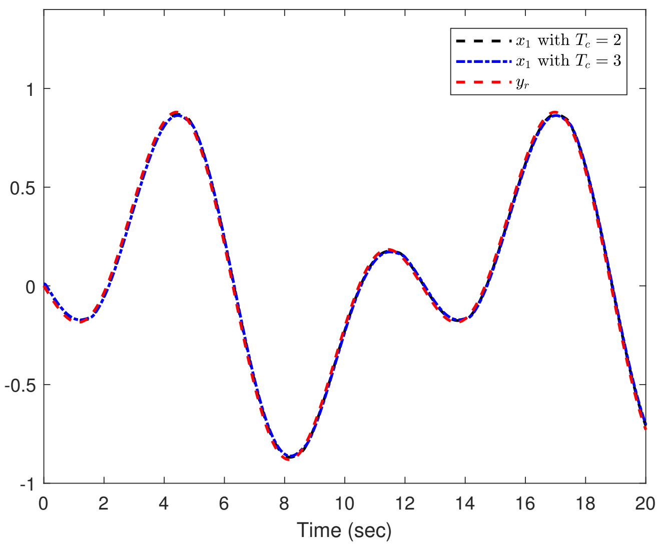

Figure 9. System output y and reference signal y_r of Example 2.

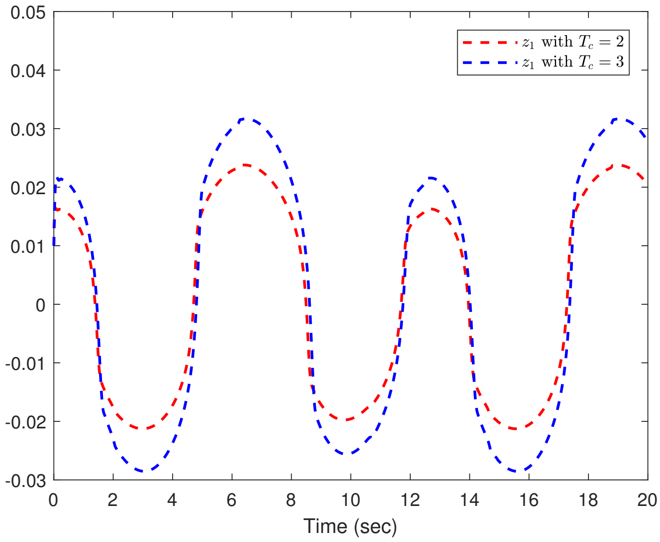

Figure 10. Tracking error z_1 of Example 2.

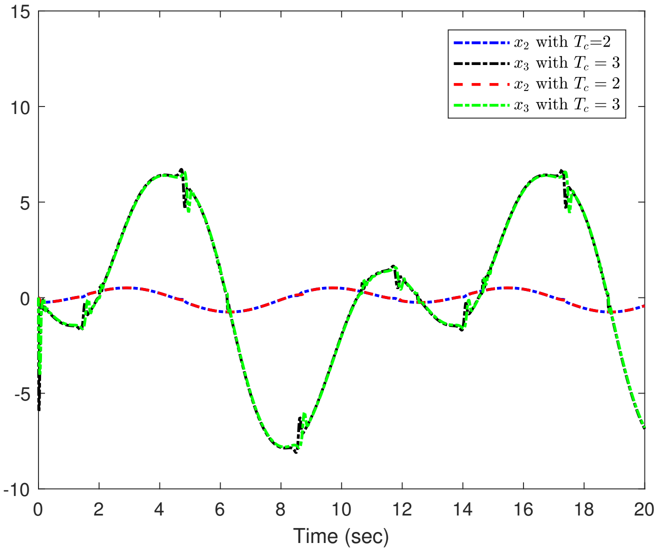

Figure 11. State variable x_2 of Example 2.

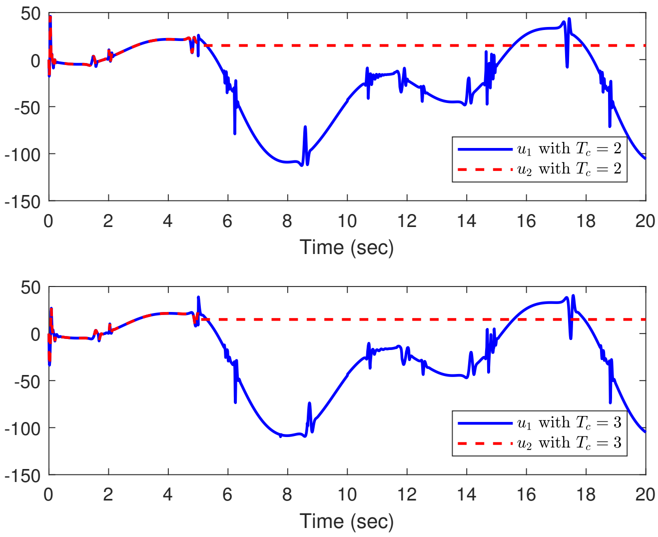

Figure 12. The actual control inputs u_1 and u_2 of Example 2.

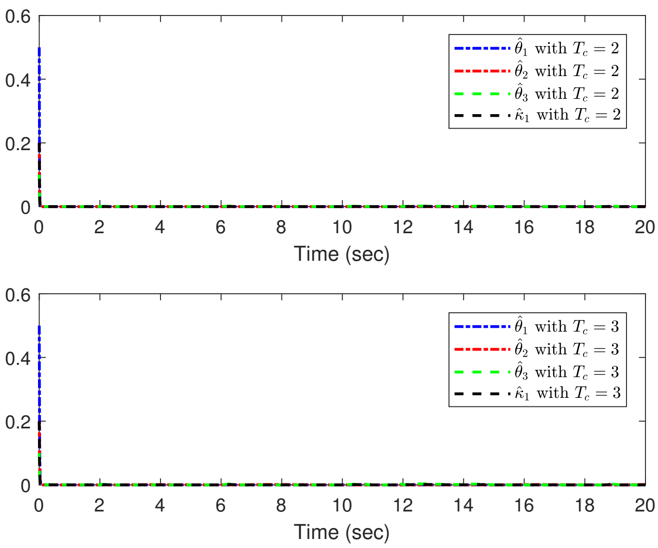

Figure 13. Adaptive laws $\hat{\theta}_1$, $\hat{\theta}_2$ and $\hat{\kappa}$ of Example 2.

Therefore, Examples 1 and 2 demonstrate the effectiveness of the control strategy presented in this paper.

5. Conclusions

In this research, the predefined time and accuracy adaptive fault-tolerant control problem has been investigated for a class of strict-feedback nonlinear systems with multiple faults. FLSs were employed to model the unknown parts of the systems. Based on the predefined time theory, a condition has been proposed that enables the tracking error to converge to the expected accuracy within predefined time while avoiding singularity issues. Combined with the backstepping mechanism, an adaptive fault-tolerant control strategy has been presented. The controller can ensure that all signals in the closed-loop system are bounded, and the tracking error meets the requirements of predefined accuracy and time. The results of two numerical simulation examples proved the effectiveness of the presented control strategy.

In addition, in future learning and research, we will extend the control strategy proposed in this article to fractional-order systems.

Author Contributions: Conceptualization, Y.S. and Y.J.; methodology, Y.S.; software, Y.J.; validation, Y.J.; formal analysis, Y.J.; investigation, Y.J.; writing—original draft preparation, Y.J.; writing—review and editing, Y.J., M.T. and H.W.; supervision, Y.S. and H.W. All authors have read and agreed to the published version of the manuscript.

Funding: This research received no external funding.

Data Availability Statement: The data presented in this study are available on request from the corresponding author. The data are not publicly available due to no datasets were generated or analyzed during the current study.

Conflicts of Interest: The authors declare no conflicts of interest.

References

1. Ma, J.; Zheng, Z.; Li, P. Adaptive dynamic surface control of a class of nonlinear systems with unknown direction control gains and input saturation. *IEEE Trans. Cybern.* **2015**, *45*, 728–741. [CrossRef]
2. Zhou, J.; Wen, C.; Wang, W.; Yang, F. Adaptive backstepping control of nonlinear uncertain systems with quantized states. *IEEE Trans. Autom. Control* **2019**, *64*, 4756–4763. [CrossRef]
3. Tang, G.; Dong, R.; Gao, H. Optimal sliding mode control for nonlinear systems with time-delay. *Nonlinear Anal. Hybrid Syst.* **2008**, *2*, 891–899. [CrossRef]
4. Xu, N.; Zhao, X.; Zong, G.; Wang, Y. Adaptive control design for uncertain switched nonstrict-feedback nonlinear systems to achieve asymptotic tracking performance. *Appl. Math. Comput.* **2021** , *408*, 126344. [CrossRef]
5. Wang, C.; Wen, C.; Hu, Q. Event-triggered adaptive control for a class of nonlinear systems with unknown control direction and sensor faults. *IEEE Trans. Autom. Control* **2020**, *65*, 763–770. [CrossRef]
6. Jiang, D.; Jiang, W.; Zhu, X.; Yin, X. Adaptive control for full-states constrained nonlinear systems with unknown control direction using barrier Lyapunov functionals. *Trans. Inst. Meas. Control* **2022**, *44*, 2967–2977. [CrossRef]
7. Chen, B.; Lin, C.; Liu, X.; Liu, K. Adaptive fuzzy tracking control for a class of MIMO nonlinear systems in nonstrict-feedback form. *IEEE Trans. Cybern.* **2015**, *45*, 2744–2755. [CrossRef]
8. Ma, J.; Xu, S.; Zhuang, G.; Wei, Y.; Zhang, Z. Adaptive neural network tracking control for uncertain nonlinear systems with input delay and saturation. *Int. J. Robust Nonlinear Control* **2020**, *30*, 2593–2610. [CrossRef]
9. Sun, W.; Su, S.; Wu, Y. Novel adaptive fuzzy control for output constrained stochastic nonstrict feedback nonlinear systems. *IEEE Trans. Fuzzy Syst.* **2020**, *29*, 1188–1197. [CrossRef]
10. He, Y.; Chang, X.; Wang, H. Command-filtered adaptive fuzzy control for switched MIMO nonlinear systems with unknown dead zones and full state constraints. *Int. J. Fuzzy Syst.* **2023**, *25*, 544–560. [CrossRef]
11. Yu, T.; Liu, Y.; Liu, L. Adaptive fuzzy control of nonlinear systems with function constraints based on time-varying IBLFs. *IEEE Trans. Fuzzy Syst.* **2022**, *30*, 4939–4952. [CrossRef]
12. Li, M.; Xiang, Z. Adaptive neural network tracking control for a class of switched nonlinear systems with input delay. *Neurocomputing* **2019**, *366*, 284–294. [CrossRef]
13. Yang, D.; Zong, G.; Liu, Y.; Choon, K. Adaptive neural network output tracking control of uncertain switched nonlinear systems: An improved multiple Lyapunov function method. *Inf. Sci.* **2022**, *606*, 380–396. [CrossRef]
14. Wang, H.; Chen, B.; Lin, C.; Sun, Y. Observer-based adaptive neural control for a class of nonlinear pure-feedback systems. *Neurocomputing* **2016**, *171*, 1517–1523. [CrossRef]

15. Liu, J.; Jiang, Y. Adaptive fuzzy control for high-order nonlinear systems with time-varying full-state constraints and input saturation. *Int. J. Adapt. Control Signal Process.* **2023**, *37*, 710–725. [CrossRef]
16. Zhang, J.; Yang, G. Robust adaptive fault-tolerant control for a class of unknown nonlinear systems. *IEEE Trans. Ind. Electron.* **2017**, *64*, 585–594. [CrossRef]
17. Zhang, H.; Cui, Y.; Wang, Y. Hybrid fuzzy adaptive fault-tolerant control for a class of uncertain nonlinear systems with unmeasured states. *IEEE Trans. Fuzzy Sys.* **2017**, *25*, 1041–1050. [CrossRef]
18. Wang, J.; Pan, H.; Sun, W. Event-triggered adaptive fault-tolerant control for unknown nonlinear systems with applications to linear motor. *IEEE/ASME Trans. Mech.* **2022**, *27*, 940–949. [CrossRef]
19. Zhang, S.; Huang, C.; Ji, K. Prescribed performance incremental adaptive optimal fault-tolerant control for nonlinear systems with actuator faults. *ISA Trans.* **2022**, *120*, 99–109. [CrossRef]
20. Li, Y.; Yang, G. Adaptive asymptotic tracking control of uncertain nonlinear systems with input quantization and actuator faults. *Automatica* **2016**, *72*, 177–185. [CrossRef]
21. Wang, Y.; Xu, N.; Liu, Y. Adaptive fault-tolerant control for switched nonlinear systems based on command filter technique. *Appl. Math. Comput.* **2021**, *392*, 125725. [CrossRef]
22. Zhang, Z.; Wen, C.; Xing, L.; Song, Y. Event-triggered adaptive control for a class of nonlinear systems with mismatched uncertainties via intermittent and faulty output feedback. *IEEE Trans. Autom. Control* **2023**, *68*, 8142–8149. [CrossRef]
23. Jia, F.; He, X. Adaptive fault-tolerant tracking control for discrete-time nonstrict-feedback nonlinear systems with stochastic noises. *IEEE Trans. Autom. Sci. Eng.* **2023**, 1–13. [CrossRef]
24. Zeng, X.; Shen, Q. Adaptive fault-tolerant control for high-order nonlinear systems with supervisory controllers and command filters. *Int. J. Control Autom. Syst.* **2023**, *21*, 12–19. [CrossRef]
25. Yin, S.; Gao, H.; Qiu, J.; Kaynak, O. Adaptive fault-tolerant control for nonlinear system with unknown control directions based on fuzzy approximation. *IEEE Trans. Syst. Man Cybern. Syst.* **2017**, *47*, 1909–1918. [CrossRef]
26. Qi, H.; Chen, M.; Wu, L. Adaptive fault-tolerant control of nonlinear systems based on tuning functions. *Int. J. Robust Nonlinear Control* **2023**, *33*, 6715–6733. [CrossRef]
27. Milecki, A.; Nowak, P. Review of fault-tolerant control systems used in robotic manipulators. *Appl. Sci.* **2023**, *13*, 2675. [CrossRef]
28. Ali, K.; Mehmood, A.; Iqbal, J. Fault-tolerant scheme for robotic manipulator-Nonlinear robust back-stepping control with friction compensation. *PLoS ONE* **2021**, *16*, e0256491. [CrossRef]
29. Zhai, D.; An, L.; Li, X.; Zhang, Q. Adaptive fault-tolerant control for nonlinear systems with multiple sensor faults and unknown control directions. *IEEE Trans. Neural Netw. Learn. Syst.* **2018**, *29*, 4436–4446. [CrossRef]
30. Lin, W.; Lin, C.; Sun, Z. Adaptive multiple fault detection and alarm processing for loop system with probabilistic network. *IEEE Trans. Power Deliv.* **2004**, *19*, 64–69. [CrossRef]
31. Jiang, X.; Mu, X.; Hu, Z. Decentralized adaptive fuzzy tracking control for a class of nonlinear uncertain interconnected systems with multiple faults and denial-of-service attack. *IEEE Trans. Fuzzy Syst.* **2021**, *29*, 3130–3141. [CrossRef]
32. Lin, Y.; Lu, F.; Cheng, K. Multiple-fault diagnosis based on adaptive diagnostic test pattern generation. *IEEE Trans. Comput.-Aided Des. Integr. Circuits Syst.* **2007**, *26*, 932–942. [CrossRef]
33. Li, N.; Han, Y.; He, W.; Zhu, S. A novel network-based controller design for a class of stochastic nonlinear systems with multiple faults and full state constraints. *Int. J. Control* **2023**, *97*, 651–661. [CrossRef]
34. Sun, Y.; Chen, B.; Lin, C.; Wang, H. Finite-time adaptive control for a class of nonlinear systems with nonstrict feedback structure. *IEEE Trans. Cybern.* **2018**, *48*, 2774–2782. [CrossRef]
35. Sui, S.; Chen, L.; Tong, S. Neural network filtering control design for nontriangular structure switched nonlinear systems in finite time. *IEEE Trans. Neural Netw. Learn. Syst.* **2019**, *30*, 2153–2162. [CrossRef] [PubMed]
36. Sui, S.; Chen, L.; Tong, S. Finite-time adaptive fuzzy prescribed performance control for high-order stochastic nonlinear systems. *IEEE Trans. Fuzzy Syst.* **2021**, *30*, 2227–2240. [CrossRef] [PubMed]
37. Wu, Y.; Pan, Y.; Chen, M.; Li, H. Quantized adaptive finite-time bipartite NN tracking control for stochastic multiagent systems. *IEEE Trans. Cybern.* **2021**, *51*, 2870–2881. [CrossRef]
38. Sui, S.; Chen, L.; Tong, S. Fuzzy adaptive finite-time control design for nontriangular stochastic nonlinear systems. *IEEE Trans. Fuzzy Syst.* **2019**, *27*, 172–184. [CrossRef] [PubMed]
39. Wang, H.; Bai, W.; Liu, X. Finite-time adaptive fault-tolerant control for nonlinear systems with multiple faults. *IEEE/CAA J. Autom. Sin.* **2019**, *6*, 1417–1427. [CrossRef]
40. Polyakov, A. Nonlinear feedback design for fixed-time stabilization of linear control systems. *IEEE Trans. Autom. Control* **2011**, *57*, 2106–2110. [CrossRef]
41. Sun, Y.; Zhang, L. Fixed-time adaptive fuzzy control for uncertain strict feedback switched systems. *Inf. Sci.* **2021**, *546*, 742–752. [CrossRef]
42. Mei, Y.; Li, F.; Xia, R.; Park, J.; Shen, H. Fixed-time adaptive neural tracking control for nonstrict-feedback nonlinear systems with mismatched disturbances using an event-triggered scheme. *Nonlinear Dyn.* **2023**, *111*, 5383–5400. [CrossRef]
43. Lu, K.; Liu, Z.; Wang, Y.; Chen, L. Fixed-time adaptive fuzzy control for uncertain nonlinear systems. *IEEE Trans. Fuzzy Syst.* **2021**, *29*, 3769–3781. [CrossRef]
44. Fang, X.; Fan, H.; Liu, L. Adaptive fixed-time fault-tolerant control of saturated MIMO nonlinear systems with time-varying state constrains. *Nonlinear Dyn.* **2022**, *110*, 3463–3483. [CrossRef]

45. Cui, D.; Xiang, Z. Nonsingular fixed-time fault-tolerant fuzzy control for switched uncertain nonlinear systems. *IEEE Trans. Fuzzy Syst.* **2022**, *31*, 174–183. [CrossRef]
46. Zhang, X.; Tan, J.; Wu, J. Event-triggered-based fixed-time adaptive neural fault-tolerant control for stochastic nonlinear systems under actuator and sensor faults. *Nonlinear Dyn.* **2022**, *108*, 2279–2296. [CrossRef]
47. Sanchez-Torres, J.; Sanche, E.; Loukianov, A. Predefined-time stability of dynamical systems with sliding modes. In Proceedings of the 2015 American Control Conference (ACC), Chicago, IL, USA, 1–3 July 2015. [CrossRef]
48. Wang, H.; Tong, M.; Zhao, X.; Niu, B.; Yang, M. Predefined-time adaptive neural tracking control of switched nonlinear systems. *IEEE Trans. Cybern.* **2022**, *53*, 6538–6548. [CrossRef]
49. Fu, L.; Ma, R.; Pang, H.; Fu, J. Predefined-time tracking of nonlinear strict-feedback systems with time-varying output constraints. *J. Frankl. Inst.* **2022**, *359*, 3492–3516. [CrossRef] [PubMed]
50. Jimenez-Rodriguez, E.; Munoz-Vazquez, A.; Sanchez-Torres, J.; Defoort, M.; Loukianov, A. A Lyapunov-like characterization of predefined-time stability. *Trans. Autom. Control* **2020**, *65*, 4922–4927. [CrossRef]
51. Jia, F.; Huang, J.; He, X. Predefined-time fault-tolerant control for a class of nonlinear systems with actuator faults and unknown mismatched disturbances. *IEEE Trans. Autom. Sci. Eng.* **2023**, 1–15. [CrossRef]
52. Wang, Q.; Cao, J.; Liu, H. Adaptive fuzzy fontrol of nonlinear systems with predefined time and accuracy. *IEEE Trans. Fuzzy Syst.* **2022**, *30*, 5152–5165. [CrossRef]
53. Ni, J.; Shi, P. Global predefined time and accuracy adaptive neural network control for uncertain strict-feedback systems with output constraint and dead zone. *IEEE Trans. Syst. Man Cybern. Syst.* **2021**, *51*, 7903–7918. [CrossRef]
54. Li, P.; Yang, G. Backstepping adaptive fuzzy control of uncertain nonlinear systems against actuator faults. *J. Control Theory Appl.* **2009**, *7*, 248–256. [CrossRef]
55. Tang, X.; Tao, G.; Joshi, S. Adaptive actuator failure compensation for nonlinear MIMO systems with an aircraft control application. *Automatica* **2007**, *43*, 1869–1883. [CrossRef]
56. Fekih, A. Fault-tolerant flight control design for effective and reliable aircraft systems. *J. Control Decis.* **2014**, *1*, 299–316. [CrossRef]
57. Li, Y.; He, J.; Zhang, Q.; Zhang, W.; Li, Y. Predefined-time fault-tolerant trajectory tracking control for autonomous underwater vehicles considering actuator saturation. *Actuators* **2023**, *12*, 171. [CrossRef]
58. Jimenez-Rodriguez, E.; Snchez-Torres, J.; Loukianov, A. On optimal predefined-time stabilization. *Int. J. Robust Nonlinear* **2017**, *27*, 3620–3642. [CrossRef]
59. Jimenez-Rodriguez, E.; Munoz-Vazquez, A.; Sanchez-Torres, J.; Alexander, G. Loukianov: A note on predefined-time stability. *IFAC-PapersOnLine* **2018**, *51*, 520–525. [CrossRef]
60. Jimenez-Rodriguez, E.; Sanchez-Torres, J.; Gomez-Gutierrez, D.; Alexander, G. Loukinanov. Variable structure predefined-time stabilization of second-order systems. *Asian J. Control* **2019**, *21*, 1179–1188. [CrossRef]
61. Wang, L. *Adaptive Fuzzy Systems and Control: Design and Stability Analysis*; Prentice-Hall: Englewood Cliffs, NJ, USA, 1994. [CrossRef]
62. Gang, T.; Kokotovic, P. Adaptive control of plants with unknown dead-zones. *IEEE Trans. Autom. Control* **1994**, *39*, 59–68.
63. Cao, J.; Li, R. Fixed-time synchronization of delayed memristor-based recurrent neural networks. *Sci. China Inform. Sci.* **2017**, *60*, 032201. [CrossRef]
64. Wang, C.; Lin, Y. Decentralized adaptive tracking control for a class of interconnected nonlinear time-varying systems. *Automatica* **2015**, *54*, 16–24. [CrossRef]
65. Qian, C.; Lin, W. Non-Lipschitz continuous stabilizers for nonlinear systems with uncontrollable unstable linearization. *Syst. Control Lett.* **2001**, *42*, 185–200. [CrossRef]
66. Sun, Y.; Wang, F.; Liu, Z.; Zhang, Y.; Chen, C. Fixed-time fuzzy control for a class of nonlinear systems. *IEEE Trans. Cybern.* **2020**, *52*, 3880–3887. [CrossRef]